RESEARCH PAPER

PROJECTION OF REGIONAL CLIMATE CHANGE FOR 2023–2064 IN THE NORTHERN PART OF THE WESTERN RUSSIAN ARCTIC: A SUPPORT FOR RUSSIAN RAILWAYS

Andrey G. Kostianoy[1,2,3], Alexey D. Gvishiani[1,4], Sergey A. Lebedev[1], Igor N. Rozenberg[5], Roman I. Krasnoperov[1], Irina A. Dubchak[5], Sofia A. Gvozdik[1,6*], Olga O. Shevaldysheva[1], Vladimir N. Sergeev[1], Julia I. Nikolova[1]

[1]Geophysical Center of the Russian Academy of Sciences, Molodezhnaya Ulitsa, 3, Moscow, 119296, Russia
[2]Shirshov Institute of Oceanology of the Russian Academy of Sciences, Nakhimovskiy Ave, 36, Moscow, 117218, Russia
[3]S.Yu. Witte Moscow University, 2nd Kozhukhovskiy Proyezd, 12, Moscow, 115432, Russia
[4]Schmidt Institute of Physics of the Earth of the Russian Academy of Sciences, Bolshaya Gruzinskaya St, 10, Moscow, 123242, Russia
[5]Russian University of Transport, Obraztsova St, 9, Bldg 9, Moscow, 127055, Russia
[6]Department of Earth and Environmental Sciences, University of Milano-Bicocca, Piazza della Scienza, 4, Milano, 20126, Italy
***Corresponding author:** s.gvozdik@gcras.ru
Received: July 22nd 2025 / Accepted: November 12nd 2025 / Published: December 31st 2025
https://doi.org/10.24057/2071-9388-2025-4179

ABSTRACT. Observed climate change has significantly impacted land transportation infrastructure, including roads, railways, bridges, seaport facilities, runways, and other components. It also affects traffic management and the efficiency of the transport system, influencing maintenance costs, travel safety, and traffic flow speeds. This issue is particularly critical for the Arctic Zone of the Russian Federation (AZRF), which is undergoing rapid economic development. Despite its expanding technological infrastructure, the region remains highly vulnerable to the impacts of climate change. A comprehensive assessment of these environmental risks is essential to ensure sustainable regional growth. Observed and projected changes in temperature and humidity generally have adverse effects on the condition and operation of transportation infrastructure. The primary types of negative impacts linked to climate change have already emerged, and these trends are expected to intensify by the mid-21st century. This paper analyses projected climate change in the Western Russian Arctic for 2023–2064. Using the CNRM-CM6-1-HR model from Phase 6 of the Coupled Model Intercomparison Project (CMIP6), it evaluates three socioeconomic scenarios (SSP1-2.6, SSP2-4.5, SSP5-8.5). The results are compiled in an electronic atlas mapping the projected distribution of air and soil temperature, total precipitation, wind speed, and snow cover thickness. Analysis of projection revealed non-linear climate model variations, where parameter values can overlap across scenarios and change rates can be unexpectedly higher in optimistic pathways. These projections, assessed against a 1980–1989 baseline, were visualised in regional maps to detail hydrometeorological changes for 2023–2064. This analysis of regional climate change is vital for sustainably managing railway infrastructure. The results highlight a heterogeneous Arctic climate and identify potentially hazardous phenomena expected to increase in frequency and impact.

KEYWORDS: Arctic zone of the Russian Federation, climate change projection, Coupled Model Intercomparison Project, Shared Socioeconomic Pathways, geoinformation analysis, Russian Railways

CITATION: Kostianoy A. G., Gvishiani A. D., Lebedev S. A., Rozenberg I. N., Krasnoperov R. I., Dubchak I. A., Gvozdik S. A., Shevaldysheva O. O., Sergeev V. N., Nikolova J. I. (2025). Projection Of Regional Climate Change For 2023–2064 In The Northern Part Of The Western Russian Arctic: A Support For Russian Railways. Geography, Environment, Sustainability, 4 (18), 61-79
https://doi.org/10.24057/2071-9388-2025-4179

ACKNOWLEDGEMENTS: This work was funded by the Russian Science Foundation (project No. 21-77-30010-P) titled 'System analysis of geophysical process dynamics in the Russian Arctic and their impact on the development and operation of the railway infrastructure'.

Conflict of interests: The authors reported no potential conflict of interests.

INTRODUCTION

Short description of the studied region and regional transport infrastructure

The Arctic Zone of the Russian Federation (AZRF) is among the country's most dynamically growing territories. The sustainable socio-economic development of the AZRF, along with the expansion and modernisation of the region's infrastructure, is a key priority for the Russian authorities, as stated in official documents adopted in recent years (Decree of the President 2020a; Decree of the President 2020b, Executive order of the Government 2021). This includes creating several specialised industrial, economic, and transport clusters that stretch from the Kola Peninsula to Chukotka (Blanutsa 2020). In this regard, transport connectivity is a crucial issue for the sustainable development of this region. One economically feasible solution is the extensive use of the Northern Sea Route (NSR) in the Arctic Ocean, which has become one of the North's major transport corridors. The cargo turnover of the NSR significantly increased from 19.7 million tons in 2018 to 36.3 million tons in 2023, and this trend is likely to continue in the coming years (Smirnov 2025). The comprehensive strategy for NSR development up to 2035 includes expanding regional transport infrastructure, such as roads, railways, airports, and sea and river ports/terminals, which are necessary for cargo transfer at the logistics centres of the growing economic clusters (Decree of the Government 2022). However, planning and constructing transport facilities require sufficient analysis and assessment of the potential risks posed by natural hazards. These include earthquakes, underwater landslides, tsunamis, gas seeps, and climate-related geohazards (Krylov et al. 2024). Data analysis was conducted using geoinformation systems, as described in chapter 2 through the implementation of modern approaches.

Climate characteristics of the region based on previous research

As mentioned, AZRF and regional transport infrastructure are exposed to dramatic climate change, which affects all natural and socio-economic systems in the region. In 2022, the Russian Federal Service for Hydrometeorology and Environmental Monitoring (Roshydromet) stated in its 'Third Assessment Report on Climate Change and its Consequences in the Territory of the Russian Federation' that Russia's territory is warming at a rate of 0.51°C/decade, while the AZRF is warming at a rate of 0.71°C/decade (Third Assessment Report 2022). This is four times faster than the average global rate of 0.18°C/decade for the last 50 years (1973–2022) (Samset et al. 2023). A major finding of the Roshydromet Report is that, according to projections, the area occupied by near-surface permafrost in Russia's territory will decrease by about a quarter by the middle of the 21st century. By the end of the 21st century, this reduction is expected to be 40±15% and 72±20% respectively, according to the Shared Socioeconomic Pathways (SSPs) scenarios – SSP2-4.5 and SSP5-8.5, respectively (Third Assessment Report 2022). SSPs are climate change scenarios that represent projected global socioeconomic pathways up to 2100, as defined in the IPCC Sixth Assessment Report (2021).

The thawing of permafrost in the AZRF affects oil and gas, railway, road, and pipeline transport infrastructure, with economic implications in the hundreds of billions of dollars (Grebenets and Isakov, 2016; Kostianaia et al. 2021; Kostianaia and Kostianoy, 2023; Yakubovich and Yakubovich, 2019). Railway infrastructure in the AZRF operates under extremely difficult geological, climatic, and weather conditions. It is constantly affected by various external factors, leading to deformation of railway tracks, damage to bridges, and other infrastructure issues (Grebenets and Isakov 2016; Kostianaia et al. 2021; Third Assessment Report 2022). The thawing of permafrost and a significant rise in average air and soil temperatures cause further changes in the water balance of many rivers and lakes in this region. These processes intensify coastal abrasion, erosion, mudflows, floods, landslides, ground creep, rockfalls, rockslides, karst sinkholes, and snow avalanches (Grebenets and Isakov 2016; Kostianaia et al. 2021; Romanenko and Shilovtseva 2016; Third Assessment Report 2022). To adapt to rapid climate change, railway industry authorities are implementing new technological solutions in their planning, construction, and operational practices. This is a widely recognised priority in the field (Andersson-Sköld et al. 2021; Garmabaki et al. 2021; Kostianaia and Kostianoy, 2023).

In the framework of the Russian Science Foundation Project 'System analysis of geophysical process dynamics in the Russian Arctic and their impact on the development and operation of the railway infrastructure' (2021–2024, No. 21-77-30010, and 2025–2027 No. 21-77-30010-P) performed at the Geophysical Center of the Russian Academy of Sciences, an 'Electronic atlas of climatic changes in hydrometeorological parameters of the western part of the Russian Arctic for 1950–2021 as geoinformatic support of railway development' (Gvishiani et al. 2023a) has been compiled. This atlas and its second advanced version (Version 2, 2023) have been used for the analysis of climate change impact on railway infrastructure in the Western Russian Arctic from 1980 to 2021 (Gvishiani et al. 2023b).

One of the most important conclusions from this research was that climate warming in the studied area is very irregular throughout the year (by months), across different locations, and even along each section of the railway. Observed warming varied from 0.5°C to 2.6°C between 1980–1999 and 2000–2021. The rate of air temperature increase was highest in the last 20 years, reaching 0.5°C/decade. This led to a 2–4 cm reduction in snow cover thickness from 1980–1999 to 2000–2021, which is approximately 10%. Between 1980–1999 and 2000–2021, there was a significant increase in precipitation, with some months and areas experiencing changes from 25% to 50% of average values. The highest rate of precipitation growth was observed within the last 20 years, reaching 10%/decade along almost all railway sections (Gvishiani et al. 2023a; Gvishiani et al. 2023b). As part of this study, the region was considered to cover as much of the developing Russian Arctic as possible, particularly the area of railway development.

Working on this project, the authors were the first to propose using Hovmöller diagrams to chart the temporal variability of meteorological parameters along the tracks of selected railway mainlines. The analysis of these diagrams for seven railway mainlines in this region between 1980 and 2021 showed significant spatial heterogeneity of the order of 100–250 km in the form of bands, which are specific parts of the railway and persist for decades. One important conclusion from this analysis was that the spatial resolution of modern climate models often does not fully convey the variability of climate parameters depending on local geographic features. Since the spatial resolution of the models averages 100–500 km, the detected bands of spatial heterogeneity of meteorological parameters may be lost due to the coarse mesh of the models. Therefore,

the detected anomalous locations on the analysed railway mainlines must be brought under special control by railway operators, with the establishment of additional weather and technical monitoring systems, especially in regions with higher precipitation and soil humidity, greater snow depth, and stronger wind speed (Kostianoy et al. 2025).

Five main hydrometeorological parameters (air temperature, soil surface temperature, total precipitation, snow cover thickness and surface wind speed) and a climate model from the current Phase 6 of the Coupled Model Intercomparison Project (CNRM-CM6-1-HR) were selected for projecting the parameters' interannual variability for 2023–2064 (Juckes et al. 2020). Geospatial data were collected and prepared to create an electronic Atlas of projections for the main hydrometeorological parameters for the region of the northern part of the Western Russian Arctic (55°–80° N, 30°–100° E). The obtained maps were analysed to reveal the main tendencies in the future climate change of the studied region.

This paper aims to project the regional climate change for 2023–2064 in the Western Russian Arctic (55°–80° N, 30°–100° E) based on five meteorological parameters and three climate scenarios. The projection uses the CNRM-CM6-1-HR model from CMIP-6. It also aims to show the main spatial features of future regional climate change, which are of greatest interest for the operation of Russian Railways in this region.

MATERIALS AND METHODS

Overview of climatic models and scenarios

Modern studies of climate change impact assessment predominantly rely on modelling natural and socio-economic processes based on climate projections, using hydrodynamic models. For the effective use of such models, it is necessary to be confident that the uncertainty in the assessment of the corresponding consequences is not too great. This uncertainty results from both errors in impact models and differences in the climate projections used in calculations. It is important to establish which of these components is essential. For this purpose, the results obtained from calculations using several identical models are compared. The CMIP (Coupled Model Intercomparison Project) is a unique collaborative project dedicated to comparing climate models. It includes calculations with specified standardised external conditions, allowing reliance on estimates of future climate changes from the considered models (Juckes et al. 2020; Tolstykh 2016). Currently, Phase 6 of CMIP is in operation.

CMIP6 climatic models

Initially, the CMIP project was established under the guidance of the Working Group on Coupled Modelling of the World Climate Research Programme (WCRP). It began in 1995 as a comparison of several early global climate models. These models performed a set of basic experiments using atmospheric models to explore their relationship with the dynamic ocean, land surface, and thermodynamic sea ice. Since then, over five phases, the CMIP project has grown into a significant international research effort, bringing together many climate models developed by different scientific groups. An important aspect of CMIP6 is making data from various models publicly accessible in a standardised format for analysis by the wider climate community and users. The standardisation of modelling results into a specific format, along with the collection, archiving, and access to model output data through the Earth System Grid Federation, are central to the project (Eyring et al. 2016).

CMIP6 includes 23 model intercomparison projects. Each project incorporates data for various climate models that provide both historical simulations, showing past climate behaviour (1850–2014) under different conditions, and future climate change projections (from 2015 to 2100). Scenario MIP is one of the coupled climate model projects included in Phase 6 of CMIP. This project presents climate projections based on different models, relying on alternative scenarios that are directly relevant to societal challenges in mitigating, adapting to, or influencing climate change impacts. These climate projections will be based on a new set of emissions and land-use scenarios developed using Integrated Assessment Models (IAMs) and future Shared Socioeconomic Pathways (SSPs) associated with Representative Concentration Pathways (RCPs) (O'Neill et al. 2016). All simulations for the SSP1-2.6, SSP2-4.5 and SSP5-8.5 scenarios were taken from the single available ensemble member r1i1p1f2 of the CNRM-CM6-1-HR model. In this designation, r1 indicates the first realisation of initial conditions, i1 the default initialisation method, p1 the standard physics configuration, and f2 the second version of the external forcing setup recommended for this model. Stating this information explicitly is essential to ensure the reproducibility of results and their comparability with other CMIP6 simulations.

CMIP6 scenarios (Shared Socioeconomic Pathways)

Scenarios describing the possible future development of anthropogenic factors of climate change (i.e., greenhouse gases, chemically reactive gases, aerosols, and land use) following socio-economic development play a crucial role in climate research. They allow for the assessment of potential changes in the climate system, impacts on society and ecosystems, and the effectiveness of response options such as adaptation and mitigation across a wide range of future outcomes. The scenario development process began with the definition of RCPs as a set of four pathways for land use and emissions of air pollutants and greenhouse gases that cover a wide range of future outcomes until 2100.

Various scenarios were developed simultaneously. One avenue involved creating climate model projections based on four Representative Concentration Pathways (RCPs) within the Coupled Model Intercomparison Project Phase 5 (CMIP5) framework. Another avenue focused on developing alternative future pathways for Shared Socioeconomic Pathways (SSPs) and their associated emission and land use scenarios, using Integrated Assessment Models (IAMs). This was followed by an integration phase that combined climate modelling with future societal development scenarios based on SSPs for comprehensive analysis. There are five types of SSPs, distinguished by variations in population, economic growth, and urbanisation (O'Neill 2016).

SSPs describe alternative development pathways for future societies without climate change or climate policy. SSP1 and SSP5 envisage relatively optimistic development trends for human potential, with significant investments in education and healthcare, rapid economic growth, and well-functioning institutions. However, SSP5 assumes an energy-intensive economy based on fossil fuels, while SSP1 shows an increasing shift towards green energy. SSP3 and SSP4 assume more pessimistic development trends, with minor investments in education and healthcare, rapid population growth, and increased inequality. In SSP3, countries prioritise regional security, while SSP4 is dominated by significant inequality within and between

countries. Both these scenarios lead to the creation of societies highly vulnerable to climate change. SSP2 assumes a central pathway where trends maintain their historical patterns without significant deviations.

As a result, scenarios based on socio-economic development pathways and the emissions of greenhouse gases, air pollutants, and land use levels were created. For each of the 21st-century scenarios, the significance of the forcing pathway is described, as well as the rationale for the driving SSP.

SSP5-8.5: This scenario represents the upper limit of the development pathway range, based on the RCP8.5 pathway. SSP5 was chosen for this forcing pathway because it is the only SSP scenario with sufficiently high emissions to create a radiative forcing of 8.5 W/m^2 by 2100.

SSP3-7.0: This scenario represents the next stage in the development pathway range, for which the RCP7.0 pathway was chosen. SSP3 was selected because SSP3-7.0 is a scenario with significant land use changes, specifically a decrease in global forest cover, and high emissions of greenhouse gases and atmospheric pollutants, especially SO2. Furthermore, SSP3, when combined with this forcing pathway, is particularly relevant as it brings together relatively high societal vulnerability (SSP3) and relatively high forcing.

SSP2-4.5: This scenario represents the middle of the development pathway range and is based on the RCP4.5 pathway. SSP2 was chosen because its land use and aerosol pathways are not extreme compared to other SSPs, and it combines intermediate societal vulnerability with an intermediate level of forcing.

SSP1-2.6: This scenario represents the lower limit of the future development pathway range and is based on the RCP2.6 pathway. Its implementation is expected to result in an average value calculated by multiple models being significantly less than 2°C of warming by 2100, making it useful for analysing this policy target. SSP1 was chosen because it includes significant land use changes, particularly an increase in global forest cover. This scenario combines low vulnerability and low mitigation challenges, as well as a low forcing signal.

SSP1-1.9: This scenario is characterised by very low greenhouse gas emissions, with net CO_2 emissions becoming zero by 2050 and then negative (O'Neill 2016; Semyonov 2022).

Climatic models, scenarios, and hydrometeorological parameters

Selection of hydrometeorological parameters

For the analysis of future climate change, seven key hydrometeorological parameters were chosen: air temperature, total precipitation, wind speed, soil temperature, soil moisture content, air humidity, and snow cover thickness. However, for the present article, only five of these have been selected (Table 1). This choice is justified by the need to be consistent with the past climate analysis (1950–2021) conducted for this region in previous studies (Gvishiani et al. 2023a; Gvishiani et al. 2023b; Kostianoy et al. 2025). This set of parameters was discussed and approved by specialists from the Research and Design Institute of Informatization, Automation and Communications in Railway Transport of the Russian Railways, which was one of the commissioners of this work. The importance of these parameters for the operability of railways is discussed by Gvishiani et al. (2023b). Parameters such as surface air temperature, soil surface temperature, and precipitation were converted to the same units of measurement used in version 2 of the Atlas (1980–2022) (Gvishiani et al. 2023b).

Model CNRM-CM6-1-HR

Models that provided data to the shared repository of the CMIP6 project were considered. To select an appropriate model, data from 59 available options were analysed. This analysis included the following assessments: (1) the resolution of the atmospheric component; (2) the availability of data across various scenarios; (3) the availability of data for selected parameters. Information regarding the availability of datasets for different scenarios, nominal resolution, and climate scenarios can be found in a summary table on the official CMIP6 project resource on the internet (ESGF CMIP6 data holdings 2025).

Spatial resolution is one of the key parameters for preparing data for a projection Atlas. A higher resolution provides a more detailed description of the region in the end. It also cannot be worse than 0.5×0.65°, which is the same resolution used in preparing the Atlas for 1980–2022. This is necessary for comparing climate change in the considered region of AZRF. As a result, eight models from CMIP6, developed by scientific teams from China, France, Italy, Taiwan, the USA, and a joint EU team, were selected for consideration.

The CNRM-CM6-1-HR model, developed by a joint team from the National Centre for Meteorological Research (CNRM) and the European Centre for Advanced Research and Training in Scientific Computing (CERFACS) in 2017, includes the full list of selected parameters for all scenarios. It also has the highest spatial resolution (CNRM-CERFACS contribution 2025). This projection model calculates parameters from 2015 to 2100. The model is widely used in scientific research and demonstrates high reliability in assessments. It was chosen for the present analysis.

The selected model incorporates data from experiments based on four SSPs: SSP1-2.6, SSP2-4.5, SSP3-7.0, and SSP5-8.5. It also includes data from piControl (pre-industrial control experiment) and historical (historical experiment for 1850–2005) scenarios. Three illustrative scenarios were chosen for the study, characterising low, medium, and high levels of solar radiation expected by 2100: SSP1-2.6 (sustainable development scenario), SSP2-4.5 (intermediate scenario), and SSP5-8.5 (fossil fuel-intensive development).

Table 1. Hydrometeorological parameters selected for climate change projecting

Parameter	Units	CMIP6 notation	Description
Air temperature	°C	tas	Near-surface air temperature (typically 2 m)
Soil temperature	°C	ts	Temperature of the lower atmospheric layer
Total precipitation	kg/(m^2·s)	pr	Including liquid and solid phases
Snow cover thickness	m	snd	The thickness of the snow layer covering the ground. Recorded as 0.0 where ground is absent
Wind speed	m/s	sfcWind	Average near-surface wind speed (typically 10 m)

During the comparison and analysis of climatic variability, data for the 1980–1989 period were used. The MERRA-2 reanalysis (Modern-Era Retrospective Analysis for Research and Applications, Second Edition) was chosen as the dataset. Its characteristics were described in detail in our previous works (Gvishiani et al. 2023a; Gvishiani et al. 2023b; Kostianoy et al. 2025) and in the main documentation of the reanalysis (Gelaro et al. 2017).

This study relies exclusively on remote sensing data from the CMIP6 project. Records from ground-based meteorological stations were not incorporated, as validation against in-situ observations falls outside the primary focus of this research (Bocharov et al. 2025).

Visualisation of climatic data

Climatic database

The results of experiments using CMIP6 models are available in several official repositories and are open to all users. Data acquisition was carried out using the Centre for Environmental Data Analysis Archive. This archive is part of the Natural Environment Research Council Environmental Data Service and is responsible for storing atmospheric and Earth system research data. The repository follows a unified storage structure for all CMIP6 project models. Since the study was based on a comparison of data over several decades, we specifically used monthly averages (Amons) obtained using the CNRM-CM6-1-HR high-resolution climate model. This choice ensured that the temporal resolution of the dataset corresponded to monthly averages rather than daily or seasonal aggregates.

Each downloaded file contains information about a specific climate variable, scenario, and time period. The data are provided in the *.nc format (Network Common Data Form). For this study, data for the period 2023–2064 were selected using automated tools. These tools also clipped the data to the corresponding area from 30 to 100 degrees east longitude and from 55 to 80 degrees north latitude. The selection included the climate parameters described earlier and three emission scenarios. In total, over 9 GB of data were acquired as an initial dataset.

Compilation of hydrometeorological parameter maps

The further processing of the dataset can be divided into several main stages:

Stage 1: Converting *.nc files to *.grd format and forming the dataset in Surfer software.

Using data from the CNRM-CM6-1-HR model (CMIP6), grid values were calculated for each of the three scenarios and each climate parameter. The downloaded files were converted into grid format (*.grd) and compiled into a unified dataset. Monthly samples for each parameter over the period 2023–2064 were added as input data. These files were systematically saved to internal storage, each representing a raster grid with a spatial resolution of 0.5×0.5°.

Stage 2: Calculation of averaged indicators for key parameters.

For each hydrometeorological parameter, indicators were calculated to show both average projected trends over several time intervals and seasonal variations. The selected timeframes include single years, a 40-year period, two 20-year periods, and the difference between these 20-year periods to analyse trends. Seasonal trends were evaluated using data from representative months for each season: January, April, July, and October. The resulting structure of indicators for each parameter and each scenario includes:

Average projected parameter values for 2022;

Average projected parameter values for 2023–2064;

Average projected parameter values for 2023–2042;

Average projected parameter values for 2043–2064;

Average projected parameter values for January 2023–2064;

Average projected parameter values for April 2023–2064;

Average projected parameter values for July 2023–2064;

Average projected parameter values for October 2023–2064;

Projected changes in parameter between 2053–2064 and 1980–1989;

Projected changes in parameter between 2043–2064 and 2023–2042;

Average rate of change of projected parameter values for 2023–2064.

The first group of characteristics was calculated as arithmetic means over the corresponding years or months. Changes between periods were calculated as the difference between the average values of two separate intervals: 2023–2042 and 2043–2064. The rate of change was calculated as the first derivative with respect to time (X) using first-degree polynomials (rate trend) through the least squares method (Serykh and Tolstikov 2022). The rate of change (a) of a given parameter (Y) was calculated using the linear regression formula:

$$Y(X) = aX + b \quad (1)$$

Based on this, final characteristics were obtained for analysing projected climate changes. The calculations were carried out in Golden Software Surfer (version 17.1) (Golden Software 2022; Si et al. 2010), using additional tools developed for geoinformation processing.

Stage 3: Reformatting result files for GIS, assigning coordinate systems, and refining the grid resolution.

Several processing steps were followed after compiling the dataset and completing the raster calculations. First, the data grid resolution was refined to improve the quality of visualisations and create smoother output. This was done using interpolation in Surfer, increasing the resolution from 0.5×0.5° to 0.05×0.05° using kriging. This method preserves data accuracy and helps avoid artefacts when transforming gridded data, while also smoothing transitions between values (Yang et al. 2004).

The next step involved converting the dataset for use in a GIS environment to enable map creation. The final raster files were transformed into a format compatible with ESRI ArcMap (version 10.8) (Kriging 2025). The data were saved as *.flt (Esri Float Grid) files, maintaining the refined 0.05×0.05° resolution and adding geographic referencing. Additionally, for parameters related to soil conditions and snow cover thickness, the raster data were clipped to match the coastline.

Plots of interannual variability of hydrometeorological parameters

After compiling the final datasets, the next step in preparing the Atlas was the creation and setup of GIS projects in the ESRI ArcMap MXD format (Map Exchange Document). The following procedures were carried out as part of the GIS project: for each climate parameter, project trees were created within a pre-prepared layout (which included a unified map background and general legend structure), raster datasets were added, and contour lines were calculated and displayed. The next steps included formatting the final maps, applying colour palettes, styling contour lines, adding titles, and exporting the finished images. All formatting and map creation were carried out using ESRI ArcMap (version 10.8) (Bartus 2014).

For better visualisation, all climatic schemes are displayed on the digital elevation model. The GEBCO (General Bathymetric Chart of the Oceans) model (Leminkova 2020) was chosen

for the dataset as the base map. This model provides data in meters, with a grid spacing of approximately 30 metres. For this Atlas, considering the geographic location of the study area, an equidistant conic projection was selected with a central meridian at 103°.

The final maps included the current railway network in the considered region of AZRF. This allows for an assessment of the influence of regional climate change on key railway routes and provides information for planning future transport development. This layer is based on the railway network map of Russia, derived from the Digital Chart of the World dataset (originally from 1993, updated through 2002) at a 1:1,000,000 scale. The dataset was compiled by the Russian Academy of Sciences (RAS) and the International Institute for Applied Systems Analysis (IIASA), Austria (IIASA, 2002). For use in the final maps, the railway data were clipped to match the boundaries of the study area. Additionally, the route of the planned Northern Latitudinal Railway (NLR), which is currently under construction, was also included. These routes were added to the initial dataset in *.shp (Shapefile) format.

The final maps showing the projected distribution of hydrometeorological parameters were saved in TIFF (Tagged Image File Format) and later compiled into a PDF document. The following sections will present the main trends and general patterns of projected climate change based on this data. As a result, 234 maps for all 7 projected parameters have been prepared. Next, an analysis of 5 parameters will be presented, chosen as the most representative and significant (chapter 3).

RESULTS

Analysis of trends in the interannual variability of main hydrometeorological parameters

Initially, an analysis of trends and data distribution across different periods was prepared. This analysis utilised two main tools: Table 2, which summarises minimum and maximum values, linear trends, and differences between periods, and interannual variability plots (Fig. 1), which illustrate temporal evolution and emphasize divergence between the scenarios.

Table 2. Key characteristics of interannual variability of all climatic parameters under 3 climate change scenarios for different periods

Parameter	Characteristic	Unit	SSP 1-2.6	SSP 2-4.5	SSP 5-8.5
Air temperature	Linear trend 2015–2100	°C/10 years	0.24	0.58	1.01
	Linear trend 2023–2064	°C/10 years	0.29	0.93	0.77
	Average value 2022	°C	−3.02	−5.09	−3.11
	Average value 2023–2064	°C	−2.62	−2.65	−1.79
	Difference between periods (2043–2064) – (2023–2042)	°C	0.55	1.81	1.55
Total precipitation	Linear trend 2015–2100	mm/10 years	0.31	0.69	1.45
	Linear trend 2023–2064	mm/10 years	0.71	1.39	1.58
	Average value 2022	mm	49.37	45.09	48.22
	Average value 2023–2064	mm	49.65	49.18	50.16
	Difference between periods (2043–2064) – (2023–2042)	mm	1.71	2.54	3.51
Wind speed	Linear trend 2015–2100	(m/s)/10 years	0.006	0.004	-0.002
	Linear trend 2023–2064	(m/s)/10 years	0.012	0.028	0.007
	Average value 2022	m/s	5.129	5.213	5.282
	Average value 2023–2064	m/s	5.25	5.264	5.282
	Difference between periods (2043–2064) – (2023–2042)	m/s	0.006	0.036	-0.006
Soil temperature	Linear trend 2015–2100	°C/10 years	0.26	0.61	1.04
	Linear trend 2023–2064	°C/10 years	0.3	0.98	0.8
	Average value 2022	°C	−2.82	−5.00	−2.95
	Average value 2023–2064	°C	−2.40	−2.46	−1.54
	Difference between periods (2043–2064) – (2023–2042)	°C	0.56	1.9	1.6
Snow cover thickness	Linear trend 2015–2100	m/10 years	−0.0013	−0.0037	−0.009
	Linear trend 2023–2064	m/10 years	−0.0004	−0.0055	−0.004
	Average value 2022	m	0.1862	0.1851	0.1866
	Average value 2023–2064	m	0.174	0.1733	0.171
	Difference between periods (2043–2064) – (2023–2042)	m	−0.0002	−0.0116	−0.007

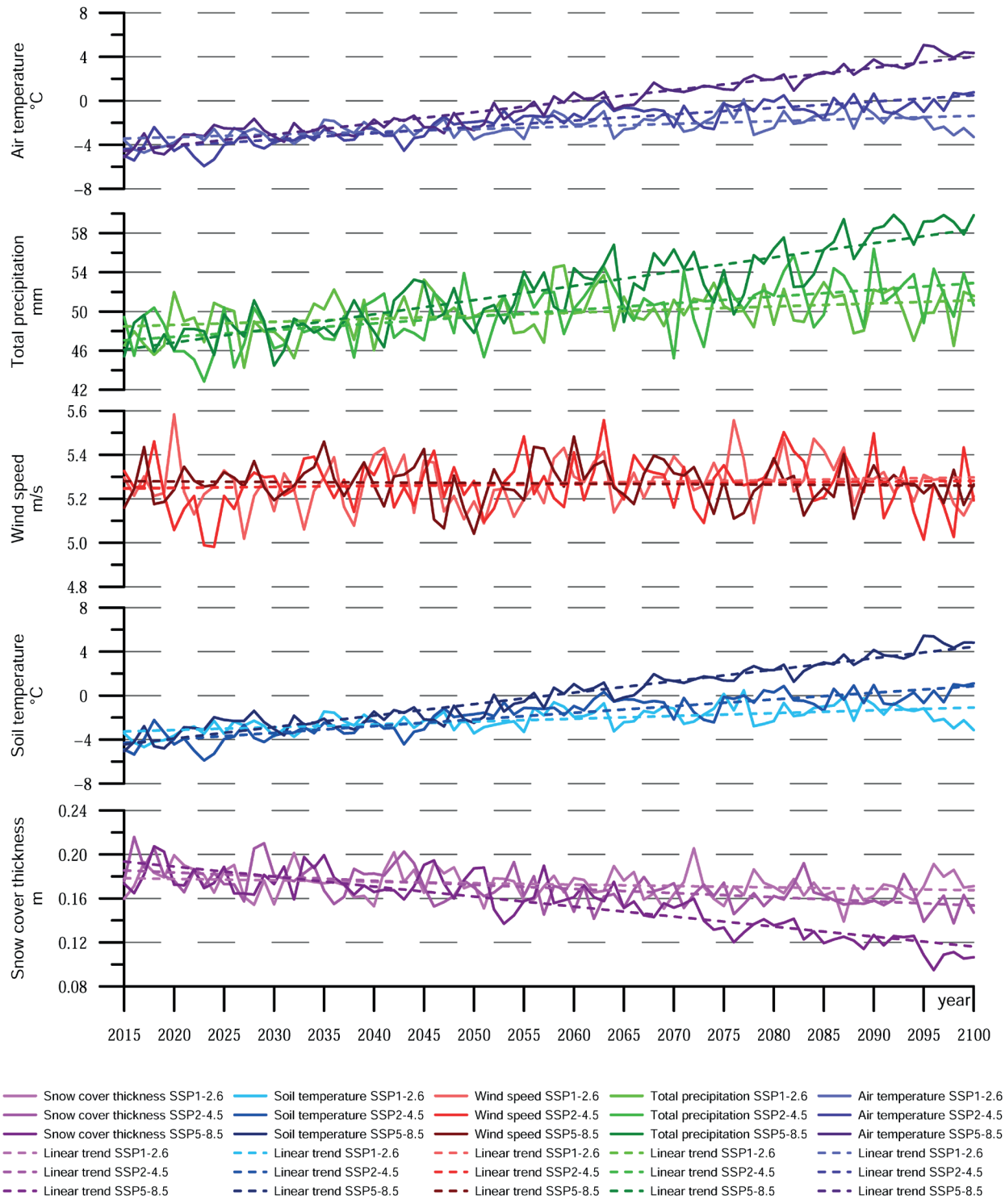

Fig. 1. Interannual variability of 5 hydrometeorological parameters in the study region under 3 climate change scenarios and their linear trends

The air temperature projection shows a consistent warming trend across all scenarios. Over the long term, from 2015 to 2100, temperature increases are estimated to be between approximately 1–2°C in the low-emission SSP1-2.6 scenario and over 8°C in the SSP5-8.5 scenario. The corresponding linear trends range from 0.24°C/decade to 1.01°C/decade. However, this increase is not uniform. In the shorter period from 2023 to 2064, the warming rate in the SSP2-4.5 scenario (0.93°C/decade) is higher than in SSP5-8.5 (0.77°C/decade). This illustrates the non-linear nature of climate dynamics and suggests that more extreme scenarios may not always show faster changes over short timescales. For instance, the average temperature in 2022 under SSP5-8.5 (–3.11°C) is similar to that under SSP1-2.6 (–3.02°C), despite their significant differences in the long term. Such periods of overlap indicate a delayed divergence and highlight the importance of monitoring changes around the middle of the century.

Precipitation trends also increase across all scenarios, though with considerable variation. By 2100, average monthly precipitation is projected to rise by ~2 mm under SSP1-2.6 and up to 12 mm under SSP5-8.5. Linear trends for 2015–2100 support this pattern, ranging from 0.31 to 1.45 mm/decade. Yet short-term rates (2023–2064) show some inversion: while SSP5-8.5 remains dominant (1.58 mm/decade), the difference with SSP2-4.5 (1.39 mm/decade) narrows. Interestingly, in 2022, the highest precipitation was recorded in SSP1-2.6 (49.37 mm), again underscoring short-term variability and possible lag effects. Even modest increases in precipitation may have significant impacts in permafrost zones, where excess surface water contributes to thermal erosion and structural instability.

Wind speed projections suggest only minor overall changes. Long-term linear trends range from +0.006 m/s/decade for SSP1-2.6 to –0.002 m/s/decade for SSP5-8.5. Across the 2023–2064 period, weak positive trends are observed in all scenarios, with the largest trend of 0.028 m/s/decade occurring in SSP2-4.5. Although absolute values are small, even slight increases can intensify mechanical stress on exposed infrastructure, particularly during peak wind events. Seasonal amplification, especially in spring, might be more critical than long-term averages.

Soil temperature trends follow a similar pattern to near-surface air temperature. Projection increase ranges from 0.26 °C/decade (SSP1-2.6) to 1.04 °C/decade (SSP5-8.5) between 2015 and 2100. In the nearer period (2023–2064), the highest warming rate is observed under the intermediate scenario SSP2-4.5 (0.98 °C/decade). This rate exceeds even the more pessimistic SSP5-8.5 (0.80 °C/decade), which again reflects temporal nonlinearity. Notably, soil temperatures under different scenarios remain relatively close until around 2070, after which divergence becomes more pronounced. From an infrastructure perspective, this projected rate of subsurface warming, approaching 1 °C every 10 years in some regions, poses a serious risk for permafrost stability. In particular, along critical corridors such as the NLR, this trend implies progressive loss of bearing capacity, increased thaw depth, and the potential for differential settlement, even within the current planning horizon.

Snow cover thickness is expected to decline gradually, from 18–20 cm in 2015 to 11–17 cm by 2100. The long-term linear trend is most negative in SSP5-8.5 (–0.009 m/decade), while SSP1-2.6 shows only minimal reductions (–0.0013 m/decade). However, intermediate periods again show different dynamics. Between 2023 and 2064, the greatest decline is observed in SSP2-4.5 (–0.0055 m/decade). Notably, the average snow cover thickness in 2022 under SSP1-2.6 was higher than under more pessimistic scenarios, and this persisted in the 2023–2064 period. These results highlight spatial and temporal differences in snow dynamics, which may influence spring flood intensity and the insulation of soils during winter.

For each hydrometeorological parameter, 33 maps were compiled to illustrate the projected variability over the period 2023–2064 under three climate change scenarios: SSP1-2.6, SSP2-4.5, and SSP5-8.5. Comparisons were also made with historical data for 1980–2021 and the year 2022 to evaluate the consistency between the historical Atlas 1980–2022 and the CNRM-CM6-1-HR model projection. We will then discuss the most significant results from the analysis of the compiled maps for each parameter.

Air temperature

Analysis of near-surface air temperature maps reveals distinct local and global trends. The spatial distribution of air temperature for 2023–2064 under both the 'optimistic' SSP1-2.6 and 'pessimistic' SSP5-8.5 scenarios indicates a northward or northeastward shift of all isotherms by 150–300 km relative to their 2022 positions. Only railway sections northeast of the Pechora–Khanty-Mansiysk line will remain, on average, within negative average annual temperatures, with the NLR area continuing to experience the most severe operational conditions. This finding is supported by seasonal temperature variability maps. For instance, January temperatures in the NLR area under both scenarios range between –20°C and –22°C, while July temperatures range from 12°C to 16°C.

Temperature increment maps comparing the periods 2043–2064 and 2023–2042 project a rise of 0.3–0.9°C under SSP1-2.6, peaking east of the Tomsk–Khanty-Mansiysk–Nadym–Yamburg line. The SSP5-8.5 scenario yields a larger increase of 1.5–1.8°C that is more spatially uniform.

Averaging over 20-year intervals somewhat smoothes the temperature change signal. The clearest projection changes for the final study decade (2053–2064) emerge when compared against the stable 1980–1989 climate baseline (Figs. 2, 3). Relative to this baseline, SSP1-2.6 projects a 2–3.5°C increase by 2053–2064, amplified in northern latitudes. SSP5-8.5 projects a greater increase (4–5°C), also peaking in the NLR area.

Calculated temperature growth rates for 2023–2064 vary regionally. They range from 0.1°C/decade in the Kazan–Perm–Yekaterinburg–Tyumen area to 0.5°C/decade in the Novy Urengoy–Igarka–Dudinka area under SSP1-2.6. Under SSP5-8.5, the rates range from 0.7 to 1.0°C/decade. Under the latter scenario, the highest rates are again projected for the Northern Latitudinal Railway sector between Salekhard and Dudinka.

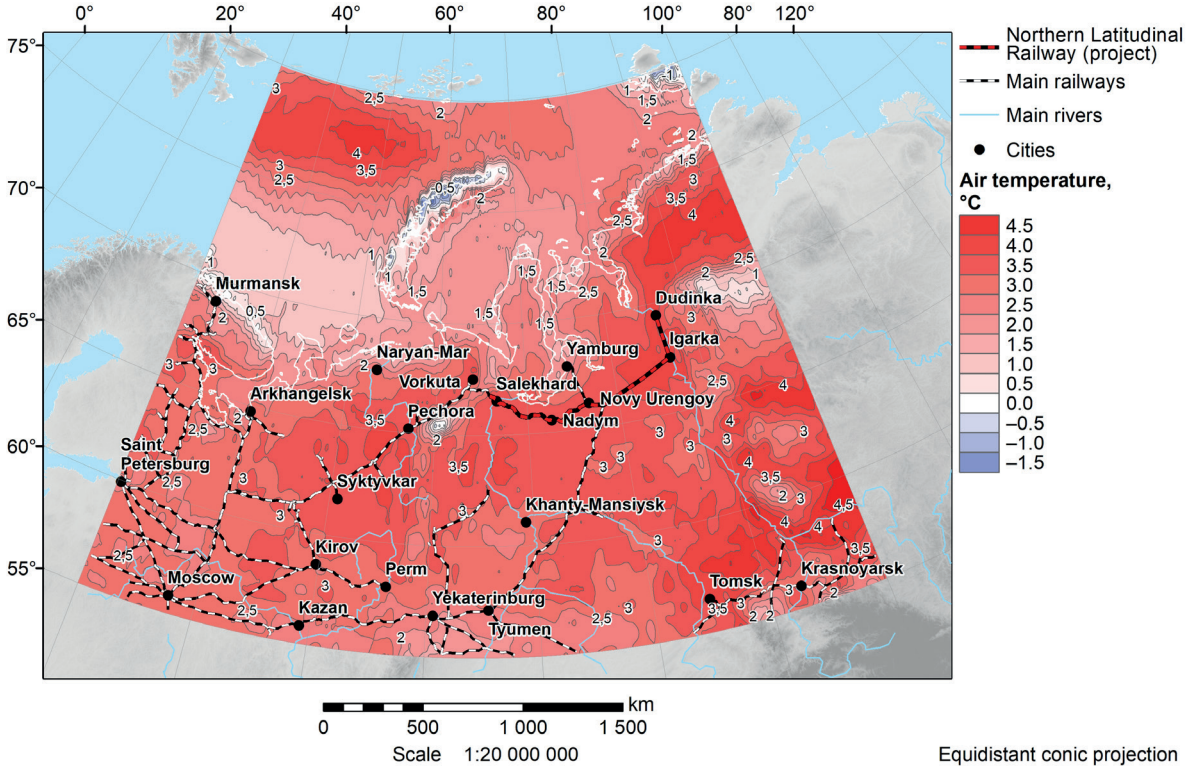

Fig. 2. Projected air temperature changes between the periods 2053–2064 (under SSP1-2.6 scenario) and 1980–1989

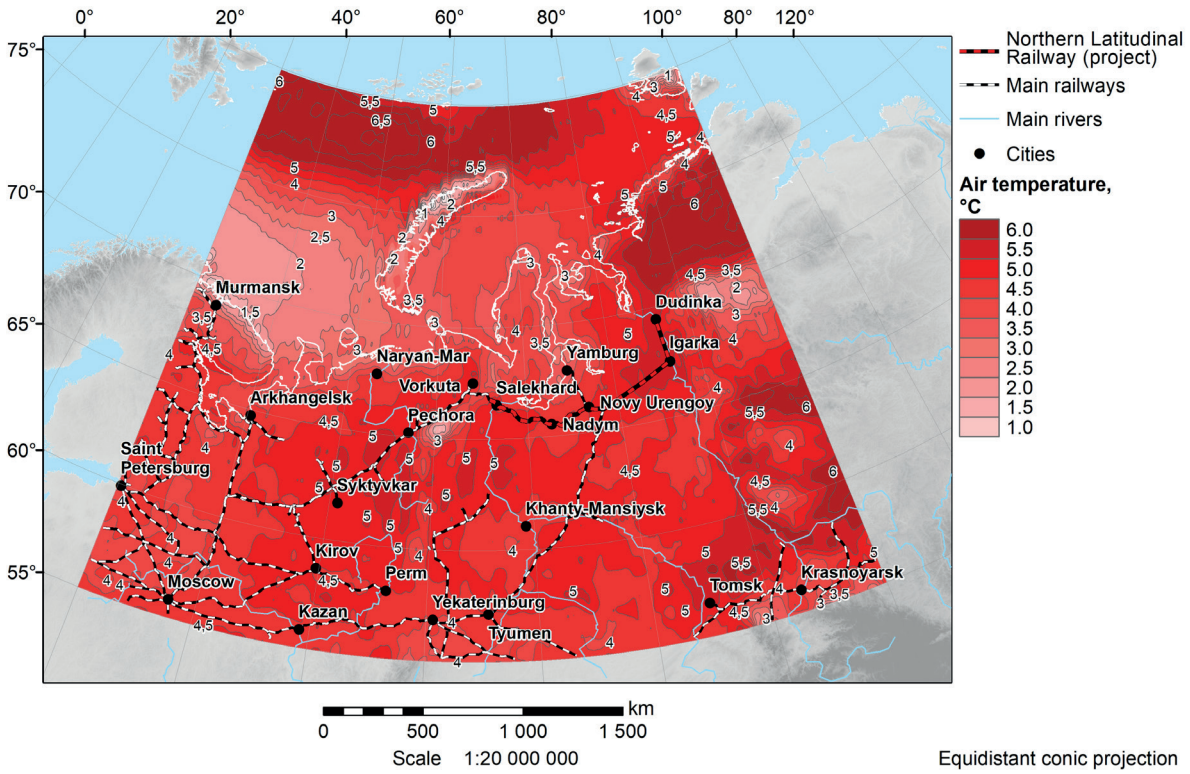

Fig. 3. Projected air temperature changes between the periods 2053–2064 (under SSP5-8.5 scenario) and 1980–1989

Total precipitation

Precipitation fields in 2022 (Fig. 4) reveal a persistent spatial pattern under all scenarios, characterised by three distinct precipitation regimes. The highest monthly totals (up to 100 mm) are concentrated in the Ural Mountains and the region east of Dudinka, while lower values (around 30–40 mm) prevail between Tomsk and Nadym. Under SSP5-8.5, this structure remains, but precipitation increases by approximately 10 mm throughout the territory, reflecting the overall intensification of the hydrological cycle.

This trend continues in the projections for 2023–2064. Under SSP1-2.6, monthly precipitation peaks at 120 mm in the western and northeastern sectors, and under SSP5-8.5, values exceed 130–135 mm. Importantly, the spatial configuration of precipitation maxima remains stable across scenarios. This suggests robust regional controls on moisture transport and orographic effects. Seasonal patterns further emphasise this amplification. In July, the most precipitation-intensive month, totals under SSP5-8.5 reach 180–200 mm in the same western and northeastern zones, which is 20–40 mm more than under SSP1-2.6. (Fig. 5) Such summer increases are particularly significant for infrastructure, as they coincide with peak active-layer thaw and can worsen surface runoff and waterlogging along railway lines.

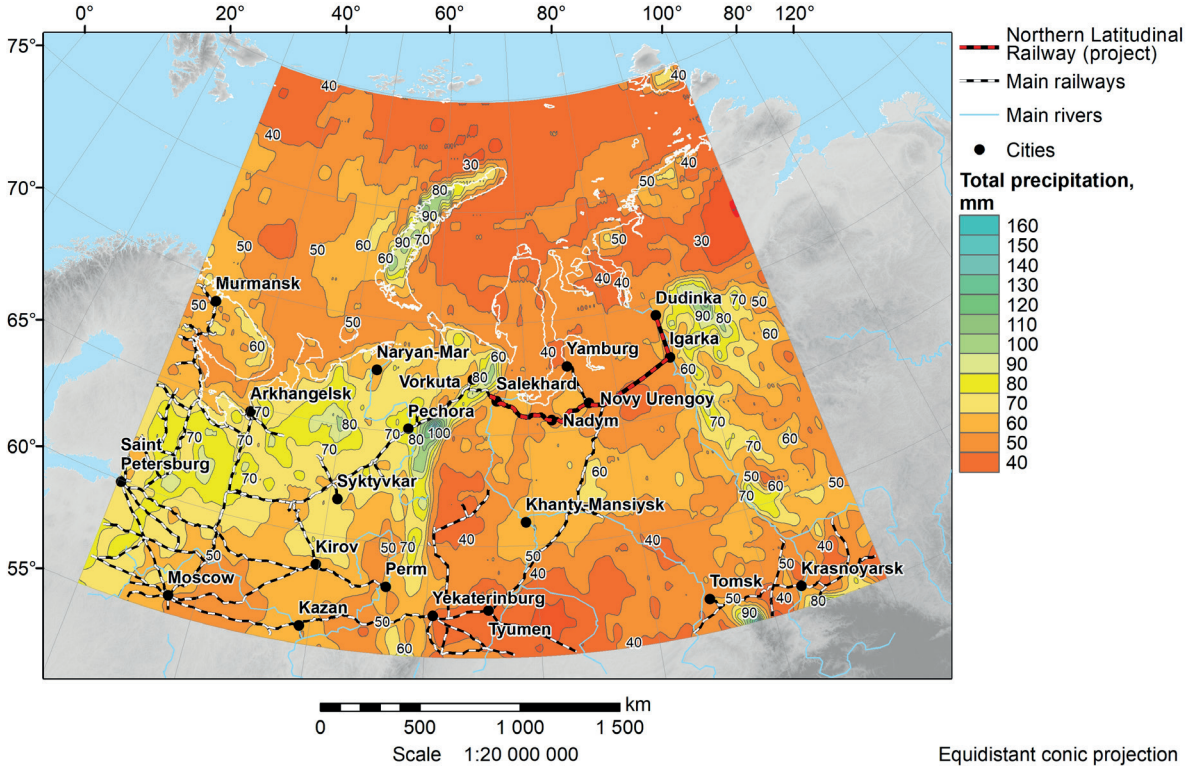

Fig. 4. Average projected total precipitation for 2022 under SSP1-2.6 scenario

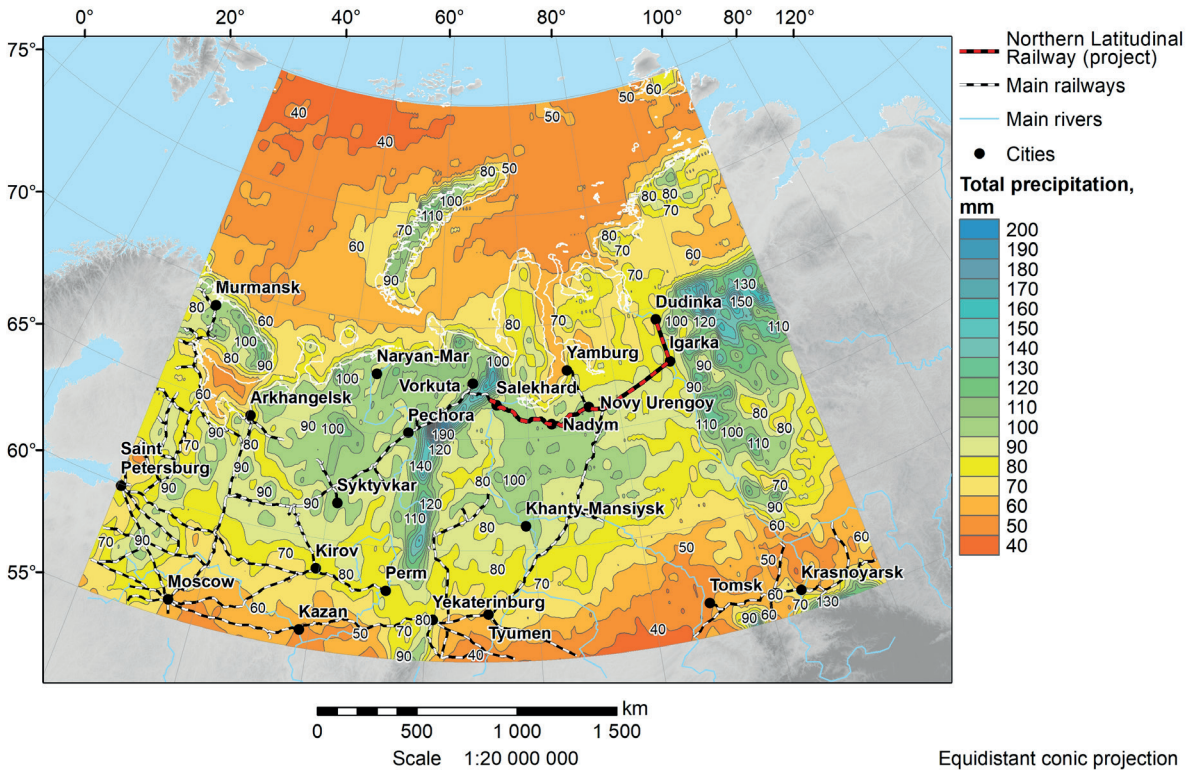

Fig. 5. Average projected total precipitation for July 2023–2064 under SSP1-2.6 scenario

Temporal comparison highlights a steady increase in precipitation across successive decades. Between 2043–2064 and 2023–2042, projection growth reaches 3–10 mm in the St. Petersburg–Yekaterinburg–Syktyvkar corridor under SSP1-2.6, and up to 17 mm under SSP5-8.5. The largest increase is concentrated in the northern Perm region and the Pechora–Vorkuta corridor, areas already prone to hydrological stress.

The long-term comparison of 2053–2064 with the baseline period of 1980–1989 (Fig. 6) confirms a marked rise in summer precipitation. Under SSP1-2.6, central regions show an increase of 10–40 mm, while SSP5-8.5 projections up to 50 mm in northern areas. These shifts suggest a growing risk of extreme rainfall events and related impacts on embankment stability and culvert capacity, especially in permafrost-affected zones.

Wind speed

Maps of spatial wind speed distribution for 2022 under both the 'optimistic' (SSP1-2.6) and 'worst-case' (SSP5-8.5) scenarios show a high degree of similarity (Fig. 7). Under both scenarios, the strongest winds, exceeding 5 m/s, are consistently observed in three regions: along the NLR corridor between Nadym and Dudinka, in the area south and southeast of Tyumen, and around St. Petersburg. In the rest of the study area, average wind speeds range from 3 to 5 m/s. Given the coincidence of high wind speeds and transport infrastructure in the Nadym–

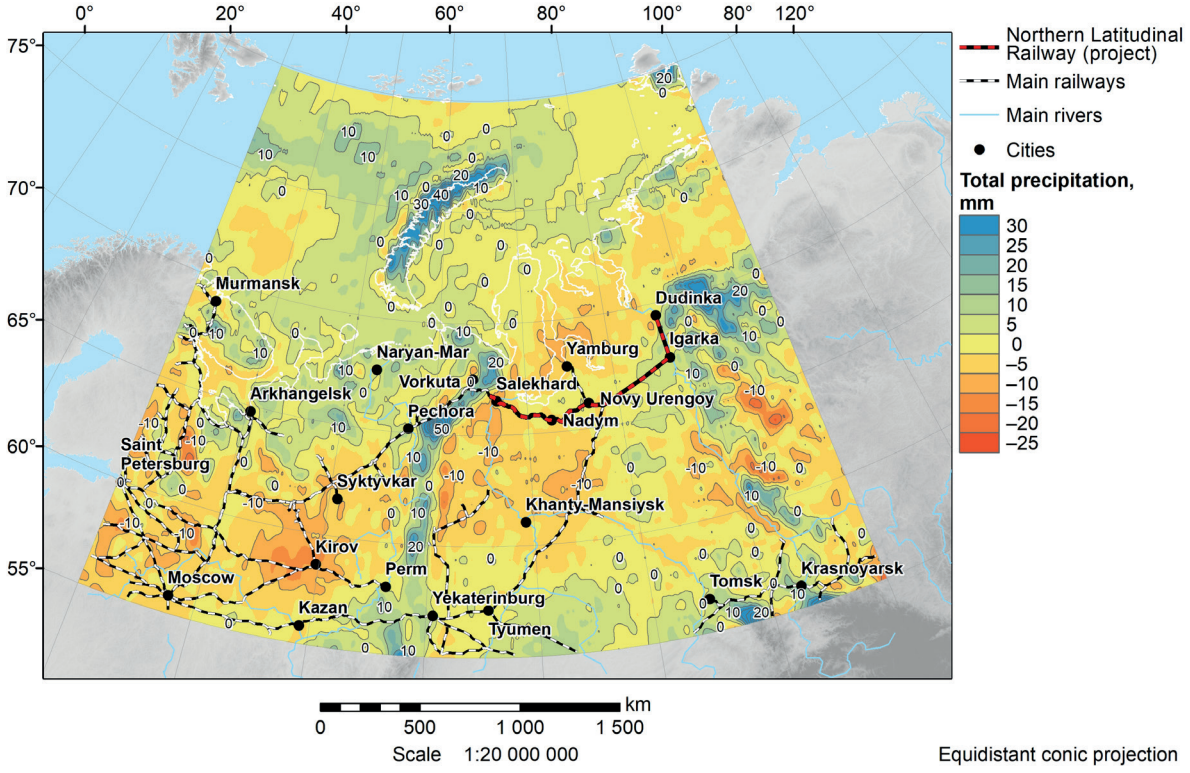

Fig. 6. Projected total precipitation changes between the periods 2053–2064 (under SSP5-8.5 scenario) and 1980–1989

Dudinka corridor, this area warrants particular attention when assessing operational risks related to wind exposure.

The average spatial distribution of wind speed over the 2023–2064 period under the same two scenarios confirms the stability of these regional patterns. The three high-wind zones previously mentioned remain clearly distinguishable. The distributions under SSP1-2.6 and SSP5-8.5 show only small differences in magnitude or extent. This persistence suggests that, unlike temperature or precipitation, wind speed in the region is controlled by stable large-scale drivers such as topography and synoptic circulation. These drivers are less affected by scenario-dependent climate forcing.

Analysis of the maps of seasonal variability of wind speeds showed that all of our selected areas persist stable throughout all months. The strongest winds occurred in spring (April), reaching 6.6 m/s at the selected track sections (Fig. 8), and the minimum wind speeds occurred in summer (July), up to 4–4.5 m/s. The same seasonal variability is observed in the rest of the study area.

Projected changes between future 20-year intervals (2043–2064 compared to 2023–2042) remain subtle. Under SSP1-2.6, a minor strengthening of 0.05–0.1 m/s is anticipated in areas such as the Moscow–Kazan transport corridor. SSP5-8.5 presents a slightly different pattern, with weak declines in northern sectors and small increases farther south. Such marginal variations are likely governed by shifts in pressure gradients, surface roughness feedbacks, and boundary-layer stability. These factors may evolve asynchronously across latitudes.

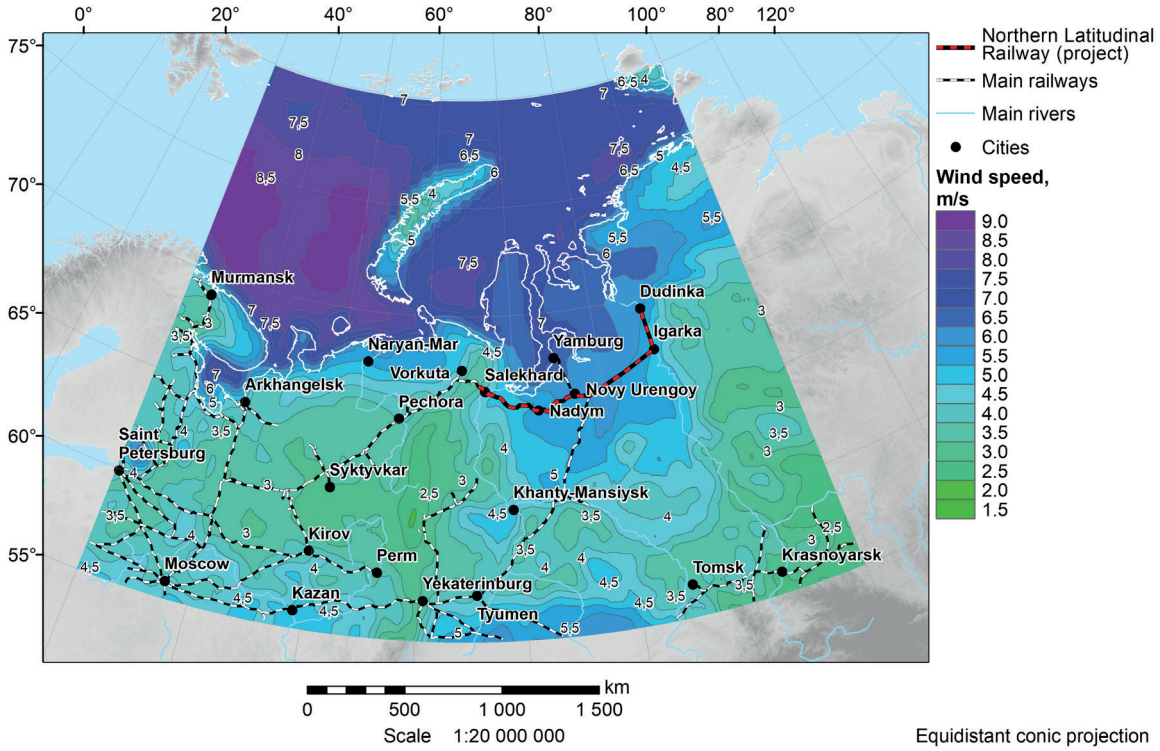

Fig. 7. Average projected wind speed for 2022 under SSP5-8.5 scenario

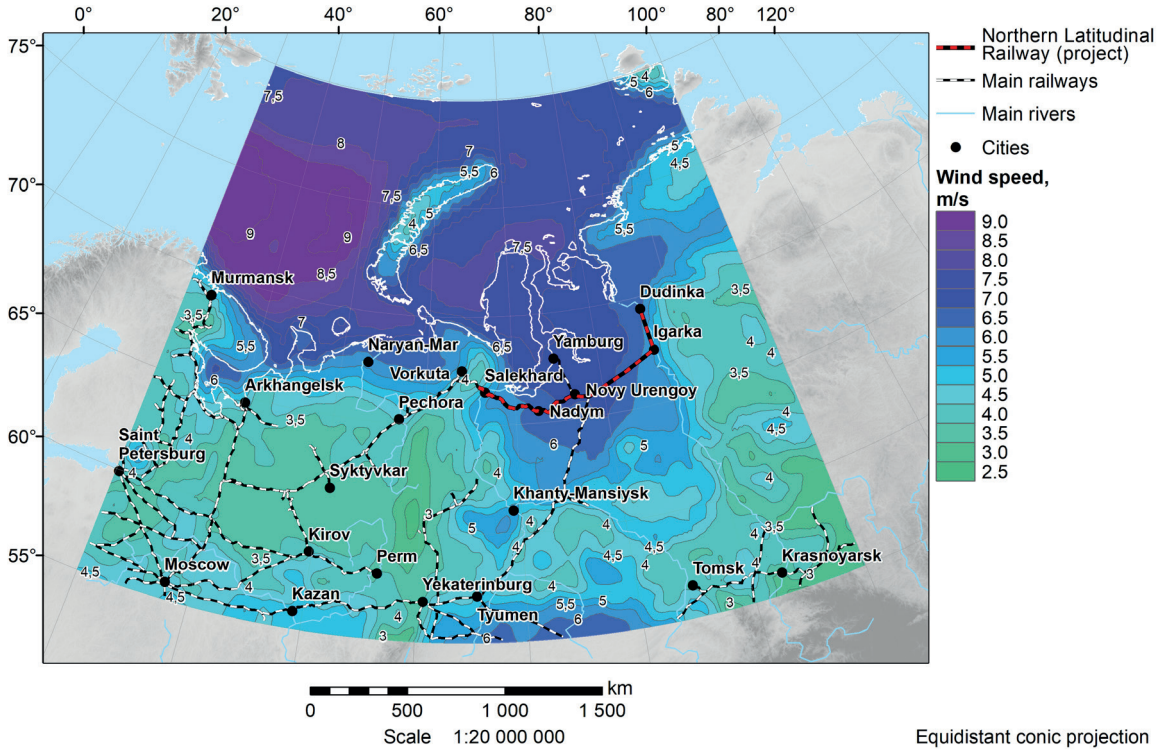

Fig. 8. Average projected wind speed for April 2023–2064 under SSP1-2.6 scenario

Projected changes in wind speed for the period 2053–2064 relative to the historical baseline of 1980–1989 are substantial in several regions (Fig. 9). According to the SSP1-2.6 scenario, average wind speeds are expected to increase by 2–3 m/s across the European sector of northwestern Russia, by 3–4 m/s in the territory between the Ural Mountains and the Yenisei River, and by 1–2 m/s east of the Yenisei. The most pronounced growth is expected along the NLR, where both topographic channelling and synoptic influences likely amplify wind intensities. Under the SSP5-8.5 scenario, the spatial pattern and magnitude of wind speed increase remain broadly comparable to those observed in SSP1-2.6. This similarity suggests that long-term wind field changes may be more strongly governed by persistent circulation regimes and orographic effects than by greenhouse gas concentration pathways alone.

Analysis of linear wind speed trends over the period 2023–2064 reveals that the most pronounced increases, ranging from 0.02 to 0.04 m/s per decade, are concentrated along the southern part of the study area. This includes the corridor from Moscow to Tomsk, as well as the stretch from Vorkuta to Dudinka along the NLR. Across the rest of the region, projected changes are negligible, with trends close to zero. Under the SSP5-8.5 scenario, however, the spatial pattern shifts. Positive wind speed trends extend across the entire area south of a notional line running from St. Petersburg through Khanty-Mansiysk to Igarka, with peak rates reaching 0.06 m/s per decade. In contrast, north of the Murmansk–Arkhangelsk–Novy Urengoy–Dudinka axis, wind speeds are projected to decrease at a similar rate (up to –0.06 m/s per decade), highlighting a spatial divergence in atmospheric circulation responses under high-emission trajectories.

Soil temperature

Figure 10 presents the spatial distribution of soil temperature in the study region for 2022 under the optimistic SSP1-2.6 scenario. The distributions for SSP2-4.5 and SSP5-8.5 are generally similar. The highest average annual temperatures (4 to 6°C) are recorded in the southwestern part of the region, while the lowest values (–4 to –14°C) are observed in the northeast under both scenarios. Among all segments of the railway network, the section from Vorkuta to Dudinka (NLR) consistently exhibits the lowest soil temperatures, indicating the need for special engineering attention.

For the period 2023–2064, the average spatial pattern of soil temperature remains largely unchanged under both scenarios. The northeastern part of the region continues to be characterised by negative temperatures. Under SSP5-8.5, however, the zero-isotherm shifts approximately 200 km north-eastward relative to SSP1-2.6. A local zone of weakly negative soil temperatures is projected to persist in the Murmansk region.

Seasonal maps indicate that the overall trend of increasing soil temperature from southwest to northeast is maintained across all scenarios and months. Figures 11 and 12 show the average soil temperature in January and July for 2023–2064 under SSP1-2.6, illustrating the seasonal amplitude. In winter, temperatures reach around –8 °C west of the Moscow–St. Petersburg corridor, and drop as low as –30 °C in the Igarka–Dudinka area (Fig. 11). In summer, the distribution aligns with latitude: 20–24 °C in the south and 12–16 °C in the north (Fig. 12).

The projected change in soil temperature between the periods 2043–2064 and 2023–2042 shows a moderate increase under SSP1-2.6. This increase is about 0.1 °C in the Yekaterinburg–Tyumen area and up to 1 °C near Igarka and Dudinka. Under the more extreme SSP5-8.5 scenario, temperature increases are substantially greater, ranging from 1.2–1.5 °C in both the central region and the Novy Urengoy–Dudinka corridor.

Long-term comparisons between 2053–2064 and the historical baseline of 1980–1989 (Fig. 13) reveal widespread warming across the study area. Under SSP1-2.6, summer soil temperatures rise by 2–3 °C across the central corridor and by up to 4 °C in southern territories. In SSP5-8.5, this warming intensifies, reaching 5–6 °C in southern zones and up to 3–4 °C in the north. These changes imply a progressive degradation of permafrost and an increasing

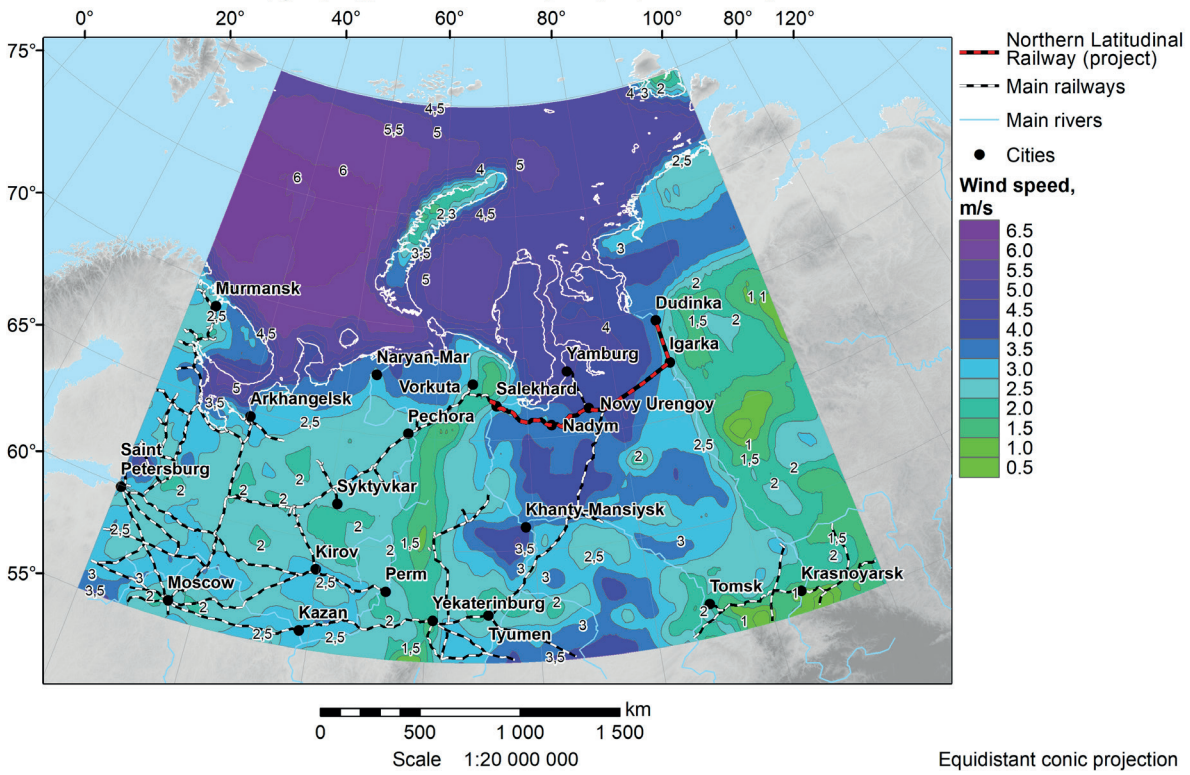

Fig. 9. Projected wind speed changes between the periods 2053–2064 (under SSP1-2.6 scenario) and 1980–1989

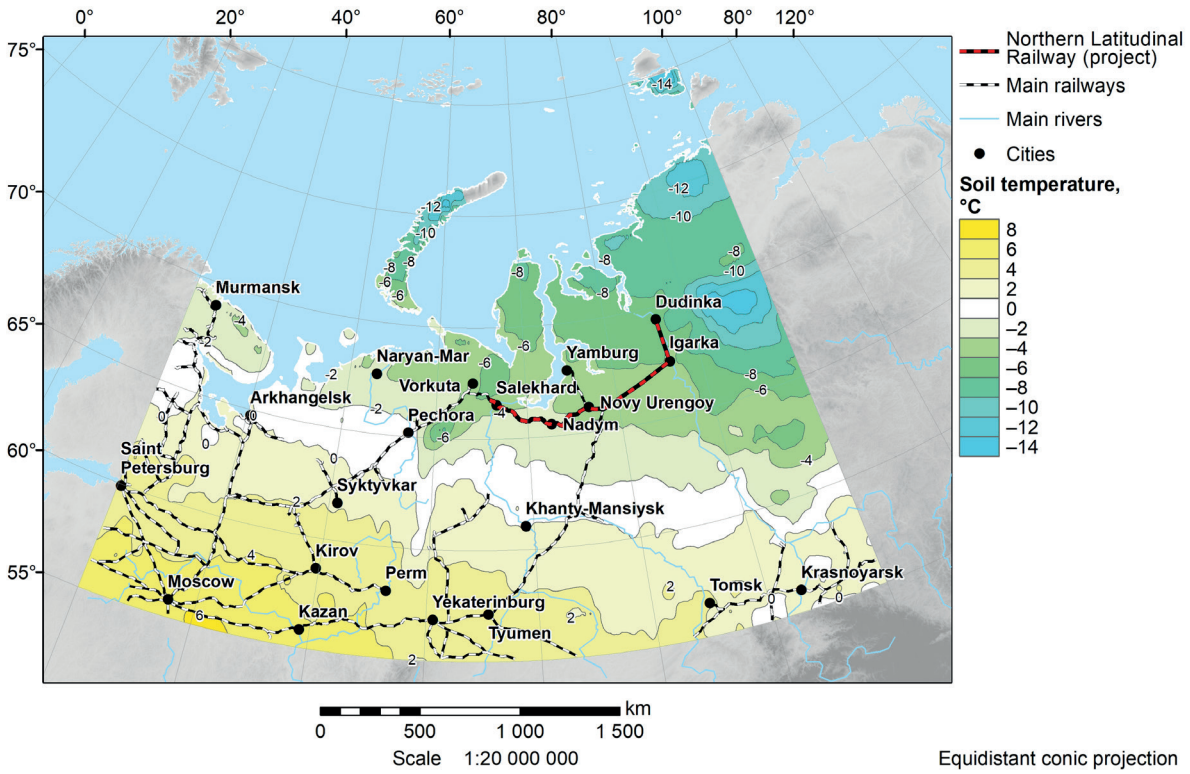

Fig. 10. Average projected soil temperature for 2022 under SSP1-2.6 scenario

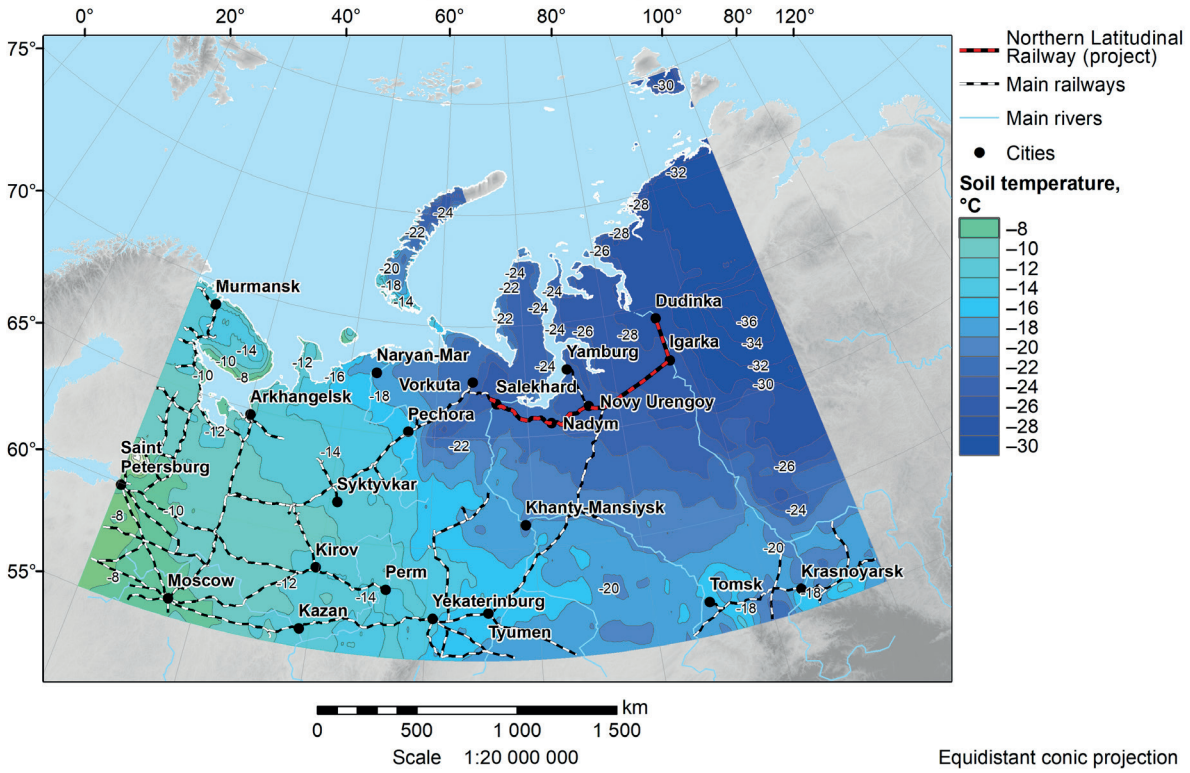

Fig. 11. Average projected soil temperature for January 2023–2064 under SSP1-2.6 scenario

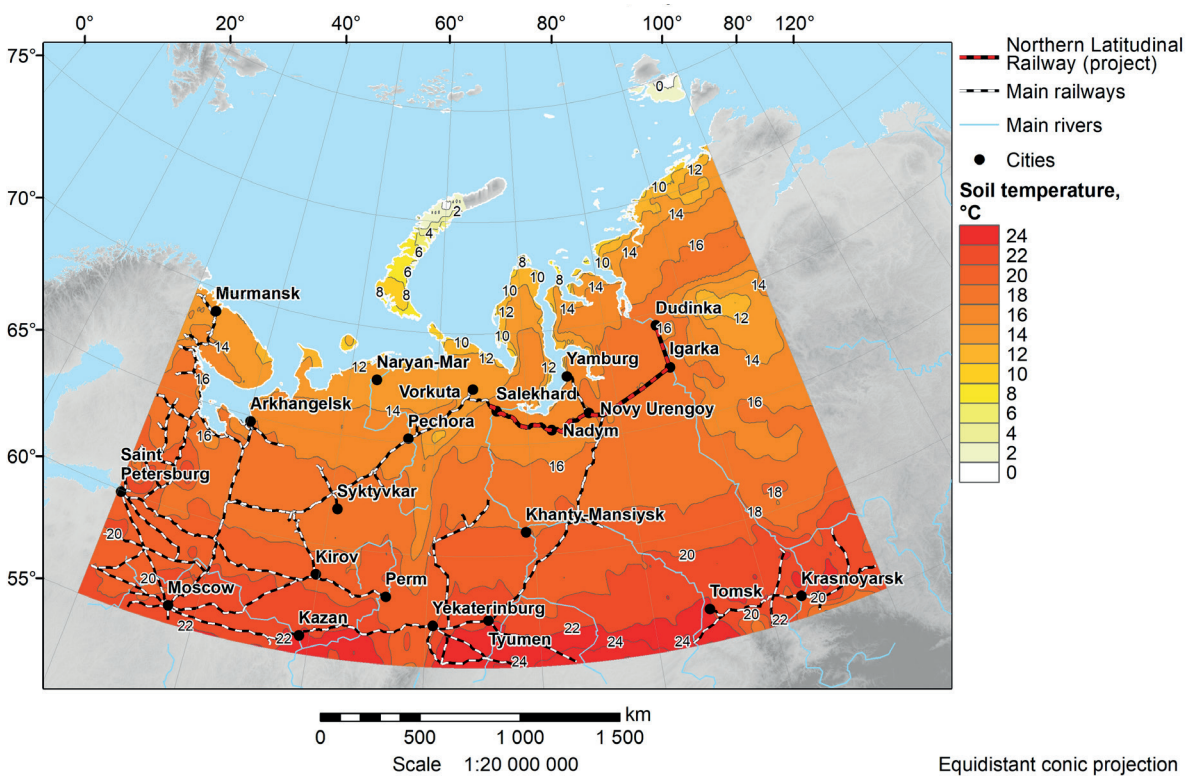

Fig. 12. Average projected soil temperature for July 2023–2064 under SSP1-2.6 scenario

depth of seasonal thaw. This may significantly affect the mechanical properties of subgrade soils along railway infrastructure.

The linear trend of soil temperature change for 2023–2064 shows that, under the SSP1-2.6 scenario, the most pronounced warming, between 0.4 and 0.55 °C/decade, is observed along the NLR between Vorkuta and Dudinka. In other parts of the study area, the warming is significantly weaker, particularly in the Perm–Yekaterinburg–Tyumen sector, where the trend ranges from 0.3 to 0 °C/decade. Under the SSP5-8.5 high-emission scenario, the warming rate increases substantially across the entire region, averaging 0.7–0.8 °C/decade. The strongest warming, from 0.8 to 1.0 °C/decade, is projected for the Novy Urengoy–Dudinka corridor (Fig. 14).

Snow cover thickness

The spatial distribution of snow cover thickness in 2022, based on both the SSP1-2.6 and SSP5-8.5 scenarios, shows a clear north-south pattern. Values increase steadily from southern to northern latitudes (Fig. 15). Snow depth is lowest, around 10 cm, in areas such as St. Petersburg–Moscow–Kazan and Yekaterinburg–Tyumen. In contrast,

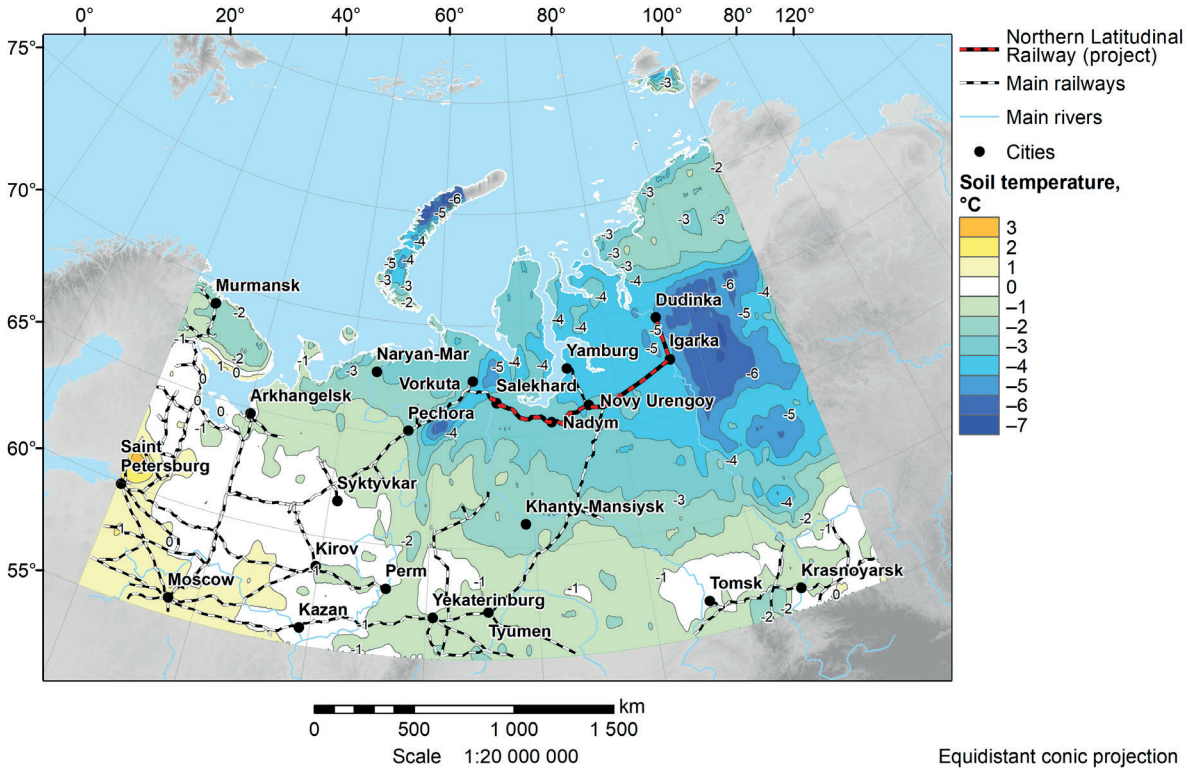

Fig. 13. Projected soil temperature changes between the periods 2053–2064 (under the SSP1-2.6 scenario) and 1980–1989

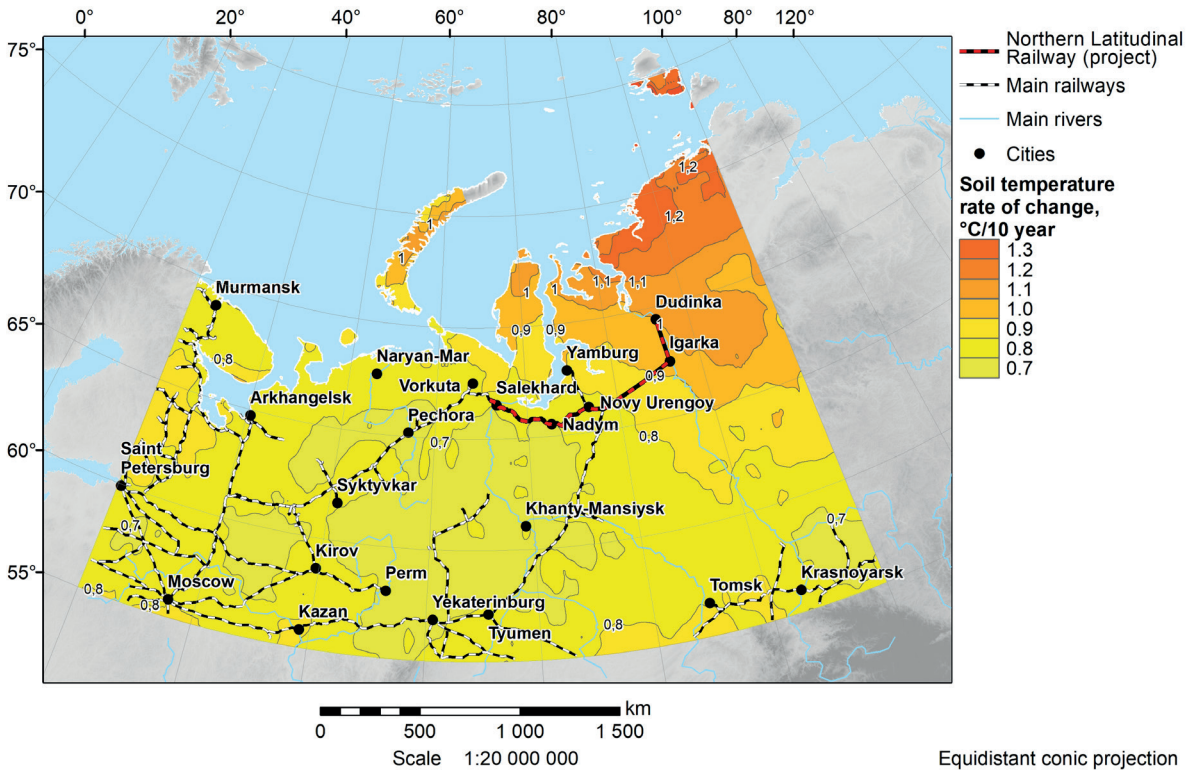

Fig. 14. Average projected soil temperature rate of change for 2023–2064 under the SSP5-8.5 scenario

the Arctic coastal zone has widespread coverage of approximately 30 cm. Furthermore, isolated regions east of Pechora and Dudinka show local accumulations reaching up to 1 m. Under SSP5-8.5, the areas with snow thickness ≤10 cm become significantly larger in both north-south and east-west directions, although the locations of local peaks remain the same.

The average distribution of snow depth projected for 2023–2064 retains these key spatial features. The southwestern part of the region continues to show minimal values (<10 cm), extending towards the White Sea coast, while snow accumulation in the northeast remains significant, up to 30 cm. The previously identified local maxima increase in area under both scenarios.

Seasonal mapping reveals that this meridional gradient in snow thickness persists regardless of the time of year or emissions pathway. Under SSP1-2.6, January snow depths during 2023–2064 range between 20 and 40 cm, with maximum values (up to 1.4 m) concentrated in the Ural Mountains and the area east of Dudinka (Fig. 16). By April, snow has largely receded from southern regions, but the same areas continue to exhibit maximum depths of up to 1.4 m.

Projected changes between the 2043–2064 and 2023–2042 periods indicate only modest variation under

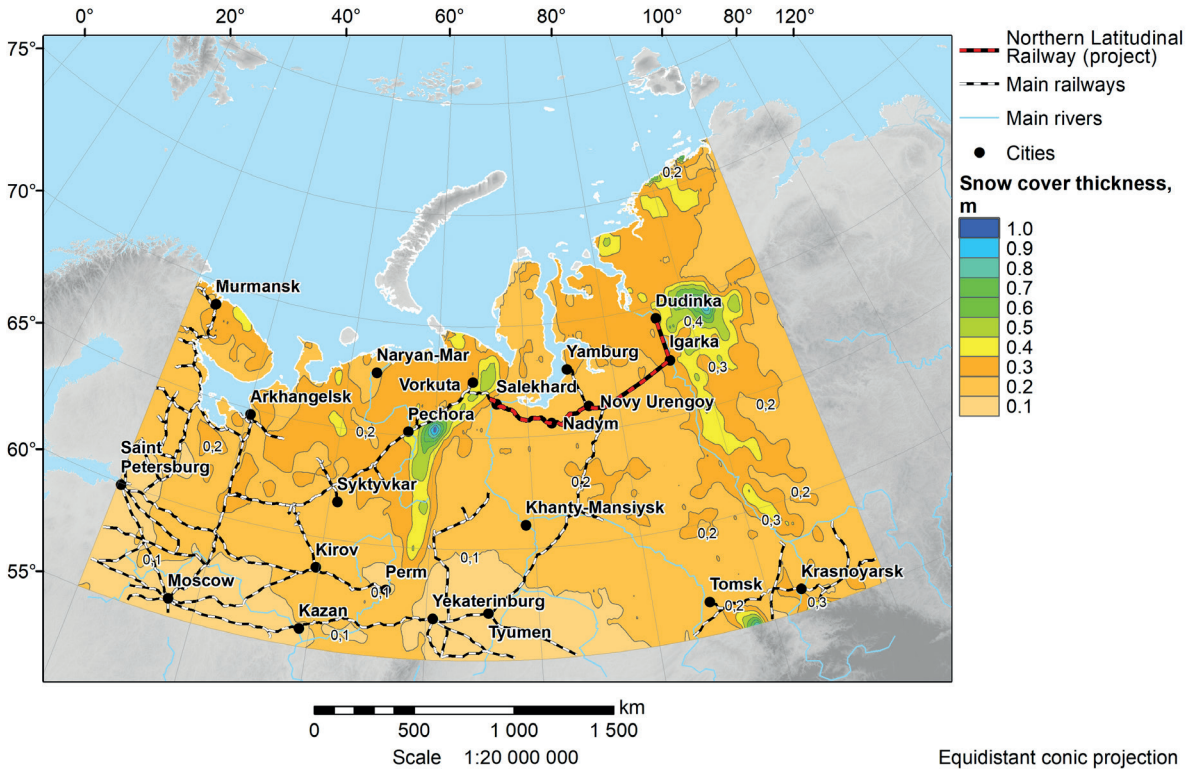

Fig. 15. Average projected snow cover thickness for 2022 under SSP1-2.6 scenario

the SSP1-2.6 scenario. Reductions of 1–2 cm are expected in western and southwestern areas, while northeastern regions may see increases of the same magnitude. Under SSP5-8.5, a more pronounced decline (up to 2.5 cm) is projected west of the Urals, while snow depth is expected to increase by 1–3 cm in eastern territories, including parts of the NLR corridor.

Long-term anomalies relative to the 1980–1989 reference period suggest that the spatial structure of snow loss is broadly similar across both scenarios, though the magnitudes vary. The most substantial reductions, ranging from 25 to 35 cm, are projected east of the Yenisei, west of the Ural Mountains, and in southern Karelia (Fig. 17).

Linear trends in snow thickness for the 2023–2064 period show distinct regional patterns. Under SSP1-2.6, the most significant reductions (0.5–1.0 cm/decade) occur in the western belt from Murmansk to Moscow, across the Pechora–Syktyvkar–Perm–Yekaterinburg–Tyumen zone, and in parts of the east-central region. Areas around Khanty-Mansiysk, Salekhard, and Nadym, as well as regions east of Igarka and Dudinka, are projected to experience slight increases, up to 0.5 cm/decade. Under SSP5-8.5, the west shows a more substantial decline (1–2 cm/decade), the central region remains relatively stable, and eastern sectors, including the NLR corridor, are expected to gain snow at a rate of 0.5–1.5 cm/decade.

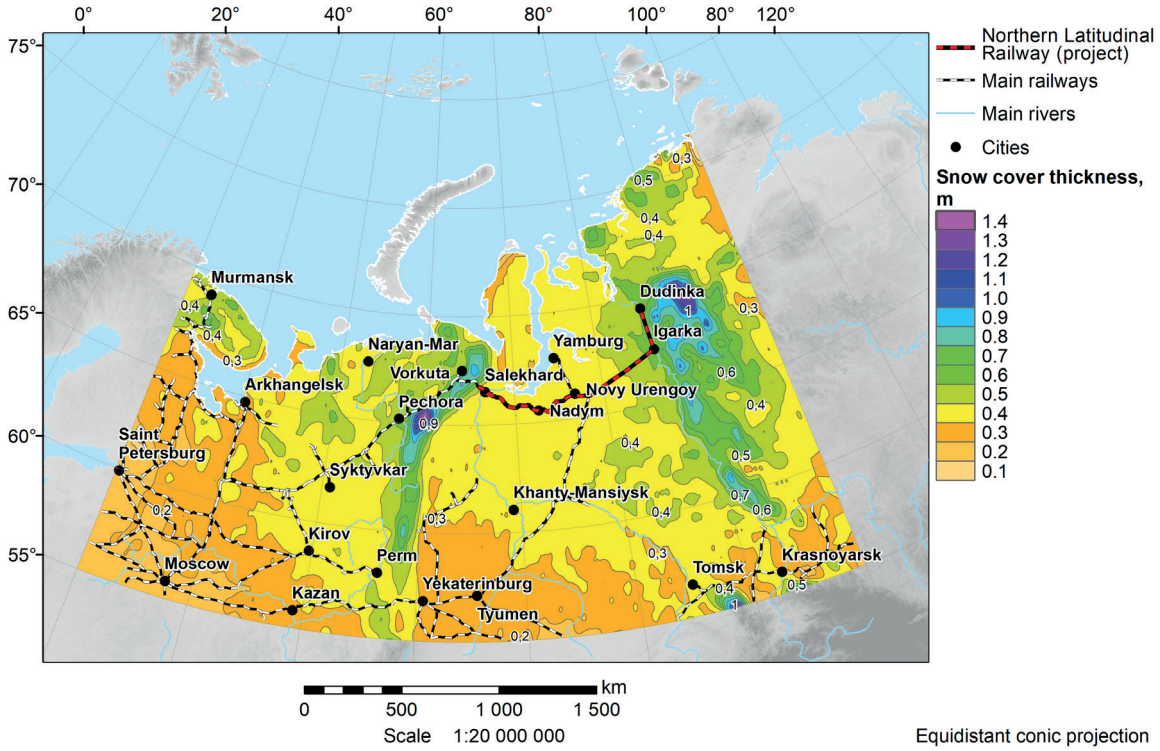

Fig. 16. Average projected snow cover thicknesses for January 2023–2064 under SSP1-2.6 scenario

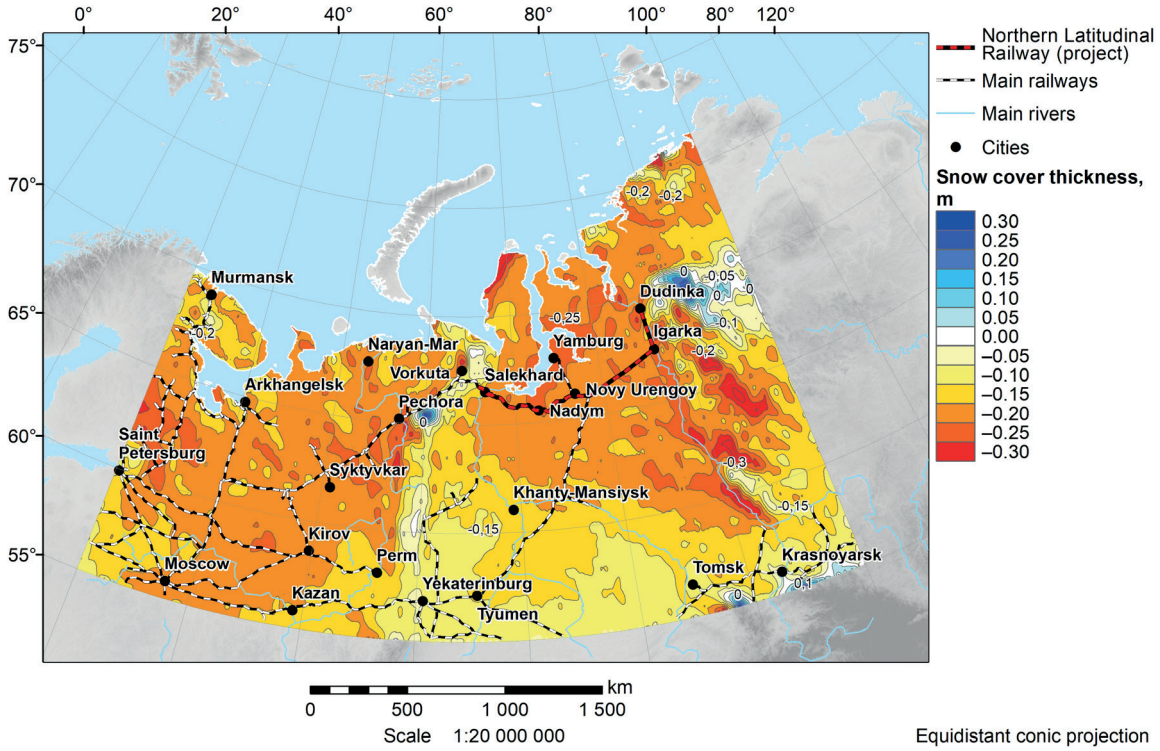

Fig. 17. Projected snow cover thickness changes between the periods 2053–2064 (under SSP5-8.5 scenario) and 1980–1989

DISCUSSION

This paper presents the results of the analysis and assessment of climate change for the region of the Western Russian Arctic (55°–80°N, 30°–100°E) for 2023–2064. The main data source for this research is Phase 6 of the Coupled Model Intercomparison Project (CMIP6), which is dedicated to comparing existing climate models (Eyring et al. 2016; Tolstykh 2016). An analysis of the CMIP6 assembly of models was performed, and in total, the characteristics of 59 models were considered. The climate model CNRM-CM6-1-HR, developed by the CNRM-CERFACS working group (France), was selected for further research. The choice of this model was justified based on the list of included hydrometeorological parameters, spatial resolution, and the availability of data for selected future climate scenarios. To select the relevant variants of the climate change model projection, three scenarios of Shared Socioeconomic Pathways (SSPs) were considered: SSP1-2.6 (sustainable development scenario), SSP2-4.5 (intermediate scenario), and SSP5-8.5 (fossil fuel-intensive development) (O'Neill et al. 2016; Semenov and Gladilshchikova 2022). Based on this data, a series of maps showing the spatio-temporal distribution of the main hydrometeorological parameters (air temperature, total precipitation, wind speed, soil temperature, and snow cover thickness) was compiled and combined into an electronic atlas.

The analysis of changes in climatic parameters and observed changes in regional climate up to 2064 has been carried out. This information is essential for the sustainable management and development of railway infrastructure. The results of the analysis emphasised the heterogeneity of climate change in the Arctic region and certain potentially hazardous phenomena. Their impact might increase in the future. For example, degradation of permafrost soils, combined with a significant increase in average temperatures, leads to changes in the balance of inland water bodies. This causes an intensification of snow and rainwater flows, and activates mudflows and landslides. These can negatively affect the existing railway infrastructure (Grebenets and Isakov, 2016; Kostianaia et al. 2021; Romanenko and Shilovtseva 2016; Yakubovich and Yakubovich 2019).

The analysis of time series for the average values of the selected parameters from 2015 to 2100 revealed considerable non-linear variations in the projected models. This indicates that for different scenarios, parameter values may overlap, and their rates of change might be lower for pessimistic scenarios compared to optimistic ones. Parameter changes were analysed relative to the established baseline period of 1980–1989, which is considered climatically stable and is commonly used for comparative climate assessments. The spatio-temporal analysis of the main hydrometeorological parameters over the period 2023–2064, performed using a compiled series of regional maps, produced the following results.

Air Temperature. It was shown that air temperature isotherms are expected to move 150–300 km north/northeast in 2023–2064 under SSP1-2.6 and SSP5-8.5 scenarios, relative to 2022. Air temperature trends for 2023–2064 vary regionally. They range from 0.1°C/decade (Kazan–Perm–Yekaterinburg–Tyumen area) to 0.5°C/decade (Novy Urengoy–Igarka–Dudinka area) under SSP1-2.6. Under SSP5-8.5, trends range from 0.7 to 1.0°C/decade. Under the latter scenario, the highest rates are again projected for the NLR sector between Salekhard and Dudinka. The continuous warming of the regional climate will lead to further thawing of permafrost soils, a change in the water balance of numerous rivers and lakes, and an intensification of geomorphological processes such as snow-water flows (a type of mudflow) and landslides. An important conclusion from the study is that objects on pile foundations with a depth of less than 6 m are at increased risk even with warming up to +2°C. Therefore, engineering protection of these objects should proceed at a faster pace than the warming of the regional climate (Grebenets, Isakov, 2016; Yakubovich, Yakubovich, 2019).

Total precipitation. A comparison of the SSP1-2.6 and SSP5-8.5 scenarios revealed that the more pessimistic scenario predicts slightly higher precipitation values west of the Ural Mountains. Between the Urals and the Yenisei, SSP5-8.5 indicated a precipitation rate approximately 10 mm higher. East of the Yenisei, the differences were more significant, with SSP5-8.5 also exceeding SSP1-2.6 by about 10 mm. The railway section in the Pechora region is likely to remain one of the most hazardous in terms of potential thawing of the railway bed in the future. Spatial variations in precipitation changes could increase regional flooding risks.

Wind Speed. Minor increases in wind speed are projected. The NLR and Tyumen regions are expected to experience the strongest winds, exceeding 5 m/s. Seasonal peaks occur in spring, reaching 6.6 m/s, which poses risks to infrastructure. The SSP5-8.5 scenario predicts a southward shift in wind speed increases. This may affect agricultural and transport systems. Intense wind activity can severely impact railway operations, causing accidents and service interruptions when trees, branches, and debris obstruct the tracks (Baker et al. 2009).

Soil temperature is a key indicator for assessing the reliability of railway performance, particularly in permafrost zones. Permafrost degradation beneath railway infrastructure can compromise the long-term stability and operational reliability of engineering structures, potentially leading to system failures. The analysis showed that warming trends in soil temperature are most severe under SSP5-8.5 (1.04°C/10 years), with the NLR area exhibiting the highest rates. For instance, in the Kola Peninsula, which has permafrost of an island nature and relatively high temperatures, Yakubovich and Yakubovich (2019) demonstrated that construction objects with foundations formed by piles of 5 m depth or less face very high risks of reduced functionality, potentially to a zero level. With a warming of up to +1°C, piles 5 m deep generally still provide functionality at U = 0.65–0.85 (where U = 1 represents the maximum functionality level). This is considered an average level of climate risk for a transport infrastructure facility. Warming up to +2°C often leads to a decrease in functionality to U < 0.5, and warming to +3°C can be considered catastrophic for construction objects, as functionality reduces to the level U = 0–0.35, which signifies an unacceptably high level of climate risks.

Snow cover thickness. Analysis of the spatial distribution and seasonal variability of snow cover thickness confirmed a consistent northward increase, applicable to all scenarios and throughout the entire snow cover period. Snow cover thickness decreases between 2053–2064 and 1980–1989 show comparable spatial distribution across scenarios, varying slightly by region. Greatest reductions (25–35 cm) are expected east of the Yenisei, west of the Urals, and in southern Karelia. Under SSP5-8.5, snow cover declines by 1–2 cm/10 years west of the Urals, remains stable in the centre, and increases by 0.5–1.5 cm/10 years in the east. These variations can alter spring flood regimes and winter transport logistics, affecting the NLR.

CONCLUSIONS

The projected changes in selected meteorological parameters from 2023 to 2064 highlight the vulnerability of the Arctic Zone of the Russian Federation (AZRF) to climate change. This is particularly true for infrastructure-heavy areas such as the Northern Latitudinal Railway. This railway, which is 707 km long, will follow the Obskaya–Salekhard–Nadym–Novy Urengoy–Korotchaevo route. Its purpose is to connect the western and eastern parts of the Yamalo-Nenets Autonomous Okrug. Rising temperatures and precipitation will challenge permafrost stability, while changes in wind and snow may disrupt transport networks. Permafrost thawing in Russia is a major concern. The market value of housing stock located solely in the permafrost area of the AZRF was over US$93 billion in 2020. This value is projected to increase to US$133.5 billion by 2055, considering buildings and infrastructure from various economic sectors planned for construction during this period (Badina 2022). Eliseev and Naumova (2019) have shown that the expected damage to motorways from permafrost degradation in the AZRF will amount to US$1.2 billion between 2020 and 2050. Therefore, developing adaptation measures for ongoing and future climate change and permafrost thawing requires an accurate projection of these changes, not only for the end of the 21st century but for each decade.

This can be achieved with the help of modern CMIP6 climate models. However, a significant challenge arises from the divergence between these models and between the SSP scenarios of global socio-economic development, which are poorly predicted. This divergence highlights the necessity for adaptive strategies that are specifically designed for different emission pathways. Policymakers must prioritise resilient infrastructure, early warning systems, and regional climate modelling to reduce potential risks. To calculate the budget required for developing adaptation measures, such as those for Russian Railways, they need the most realistic projections. Unfortunately, this is difficult to provide due to the many uncertainties associated with climate change modelling.

Our research methodology relies on a single high-resolution climate model, which may not fully capture regional characteristics. The decision to use one model, rather than an ensemble of models, places certain constraints on our findings. Given this research limitation, the focus was restricted to the selected model.

An important task is to assess ongoing climate change to understand the most likely scenario of further climate change. This will reduce the divergence between projections. We are working on this task, and it will be done by analogy with the research we recently performed for the Caspian Sea Region (Bocharov et al., 2025). Employing multi-model ensembles and local observations would refine the projection. Additional studies should consider socio-economic effects, including agricultural impacts and energy demand, to ensure sustainable development in the AZRF, including its transport infrastructure.

REFERENCES

Andersson-Sköld Y., Nordin L., Nyberg, E. and Johannesson, M. (2021). A framework for identification, assessment and prioritization of climate change adaptation measures for roads and railways. International journal of environmental research and public health, 18(23), 12314. DOI: 10.3390/ijerph182312314

Baker C. J., Chapman L., Quinn A., and Dobney K. (2009). Climate change and the railway industry: A review. Proceedings of the Institution of Mechanical Engineers, Part C: Journal of Mechanical Engineering Science, 224(3), 519–528. DOI: 10.1243/09544062JMES1558.

Bartus T. (2014). ArcGIS Desktop resources. [online] ESRI. Available at: https://www.esri.com/en-us/arcgis/products/arcgis-desktop/resources [Accessed 1 Nov. 2022].

Blanutsa V. (2021). Spatial development of the Russian Arctic Zone: analysis of two strategies. Arctic: Ecology and Economy, 11(1), 111–121 (In Russian), DOI: 10.25283/2223-4594-20211-111-121. (In Russian)

Bocharov A.V., Kostianoy A.G., Lebedev S.A., Kolomeets L.I. and Kravchenko P.N. (2025). What SSP Global Climate Change Scenario is the Caspian Sea Region Following? Part 1: Air temperature analysis. Russian Journal of Earth Sciences (in press).

CNRM-CERFACS contribution to CMIP6, (2018). CNRM-CM6-1 model: Future projections (ScenarioMIP). [online] Available at: http://www.umr-cnrm.fr/cmip6/spip.php?article11 [Accessed 26 Mar. 2024].

ESGF, (2025). CMIP6 data holdings. [online] Available at: https://pcmdi.llnl.gov/CMIP6/ArchiveStatistics/esgf_data_holdings/print_view.html [Accessed 25 Apr. 2025].

Eyring V., Bony S., Meehl G. A., Senior C. A., Stevens B., Stouffer R. J. and Taylor K. E. (2016). Overview of the Coupled Model Intercomparison Project Phase 6 (CMIP6) experimental design and organization. Geoscientific Model Development, 9, 1937–1958. DOI: 10.5194/gmd-9-1937-2016.

Garmabaki A., Thaduri A., Famurewa S. and Kumar, U. (2021) Adapting Railway Maintenance to Climate Change. Sustainability, 13(24), 13856, DOI: 10.3390/su132413856

Gelaro R., McCarty W., Suárez M. J., et al. (2017). The Modern-Era Retrospective Analysis for Research and Applications, Version 2 (MERRA-2). Journal of Climate, 30(14), 5419–5454. DOI: 10.1175/JCLI-D-16-0758.1.

Golden Software Surfer, (2022). Golden Software. [online] Available at: https://www.goldensoftware.com/products/surfer [Accessed 1 Nov. 2022].

Government of the Russian Federation, (2021). Executive order No. 3363-r of 27 Nov. 2021 on the Transport strategy of the Russian Federation until 2030 with forecast up to 2035. [online] Available at: http://static.government.ru/media/files/7enYF2uL5kFZlOOpQhLl0nUT91RjCbeR.pdf [Accessed 29 Sep. 2025]

Government of the Russian Federation, (2022). Decree No. 2115-r of 01 Aug. 2022 on approval of the Development Plan of the Northern Sea Route for the period up to 2035. [online] Available at: http://government.ru/docs/46171/ [Accessed 17 Apr. 2025].

Grebenets V. I. and Isakov V. A. (2016). Deformations of roads and railways within the Norilsk-Talnakh transportation corridor and the stabilization methods. Earth's Cryosphere, 20(2), 69-77 (In Russian).

Gvishiani A. D., Rozenberg I. N., Soloviev A. N., Kostianoy A. G., Gvozdik S. A., Serykh I. V., Krasnoperov R. I., Sazonov N. V., Dubchak I. A., Popov A. B., Kostianaia E. A. and Gvozdik G. A. (2023a). Electronic atlas of climatic changes in hydrometeorological parameters of the western part of the Russian Arctic for 1950–2021 as geoinformatic support of railway development. Applied Sciences, 13, 5278. DOI: 10.3390/app13095278.

Gvishiani A. D., Rozenberg I. N., Soloviev A. A., Krasnoperov R. I., Shevaldysheva O. O., Kostianoy A. G., Lebedev S. A., Dubchak I. A., Nikitina I. M., Gvozdik S. A., Sergeev V. N. and Gvozdik G. A. (2023b). Study of the impact of climatic changes in 1980–2021 on railway infrastructure in the Central and Western Russian Arctic based on Advanced Electronic Atlas of hydrometeorological parameters (2023b). Russian Journal of Earth Sciences, 23, ES5006. DOI: 10.2205/2023es000882.

Intergovernmental Panel on Climate Change (IPCC) (2021). Climate Change 2021: The Physical Science Basis IPCC. [online] Available at: https://www.ipcc.ch/report/ar6/wg1/ [Accessed 8 Apr. 2025].

Juckes M., Taylor K. E., Durack P. J., Lawrence B., Mizielinski M. S., Pamment A., Peterschmitt J.-Y., Rixen M. and Sénési S. (2020). The CMIP6 Data Request (DREQ, version 01.00.31). Geoscientific Model Development, 13, 201–224. DOI: 10.5194/gmd-13-201-2020.

Kostianaia E. A. and Kostianoy A. G. (2023). Railway transport adaptation strategies to climate change at high latitudes: A review of experience from Canada, Sweden and China. Transport and Telecommunication, 24(2), 180–194. DOI: 10.2478/ttj-2023-0016.

Kostianaia E. A., Kostianoy A. G., Scheglov M. A., Karelov A. I. and Vasileisky A. S. (2021). Impact of regional climate change on the infrastructure and operability of railway transport. Transport and Telecommunication, 22(2), 183–195.

Kostianoy A. G., Gvishiani A. D., Rozenberg I. B., Krasnoperov R. I., Gvozdik S. A., Lebedev S. A., Nikitina I. M., Dubchak I. A., Shevaldysheva O. O., Sergeev V. N. and Gvozdik G. A. (2025). Geoinformation analysis of regional climatic changes in the Central and Western Russian Arctic for railway development. Russian Journal of Earth Sciences, 25, ES1005. DOI: 10.2205/2025es000956.

Kriging interpolation method, (2023). Desktop ArcGIS. [online] Available at: https://desktop.arcgis.com/en/arcmap/10.3/tools/3d-analyst-toolbox/how-kriging-works.htm [Accessed 12 May 2025].

Krylov A. A., Rukavishnikova D. D., Novikov M. A., Baranov B. V., Medvedev I. P., Kovachev S. A., Lobkovsky L. I. and Semiletov I. P. (2024). The main geohazards in the Russian sector of the Arctic Ocean. Journal of Marine Science and Engineering, 12(12), 2209. DOI: 10.3390/jmse12122209.

Lemenkova P. (2020). GEBCO Gridded Bathymetry Data. [online] Available at: https://www.gebco.net/data_and_products/gridded_bathymetry_data/grid_production/ [Accessed 3 Nov. 2022].

O'Neill B. C., Tebaldi C., van Vuuren D. P., Eyring V., Friedlingstein P., Hurtt G., Knutti R., Kriegler E., Lamarque J.-F., Lowe J., Meehl G. A., Moss R., Riahi K. and Sanderson B. M. (2016). The Scenario Model Intercomparison Project (ScenarioMIP) for CMIP6. Geoscientific Model Development, 9, 3461–3482, DOI: 10.5194/gmd-9-3461-2016.

President of the Russian Federation, (2020a). Decree No. 164 of 05 Mar. 2020 on the Fundamentals of the State Policy of the Russian Federation in the Arctic until 2035. [online] Available at: http://www.kremlin.ru/acts/bank/45255 [Accessed 17 Apr. 2025].

President of the Russian Federation, (2020b). Decree No. 645 of 26 Oct. 2020 on the Strategy for the Development of the Arctic Zone of the Russian Federation and Ensuring National Security for the Period until 2035. [online] Available at: http://www.kremlin.ru/acts/bank/45972 [Accessed 17 Apr. 2025].

Romanenko F. A. and Shilovtseva O. A. (2016). Geomorphological processes in the mountains of the Kola Peninsula and climate change. Vestnik Moskovskogo Universiteta, Series 5: Geography, 6, 78–86, (In Russian).

Samset B. H., Zhou C., Fuglestvedt J. S., Lund M. T., Marotzke J. and Zelinka M. D. (2023). Steady global surface warming from 1973 to 2022, but an increased warming rate after 1990. Communications Earth & Environment, 4, 400, DOI: 10.1038/s43247-023-01061-4.

Semenov S. M. and Gladilshchikova A. A. (2022). Scenarios of anthropogenic changes in the climate system in the XXI century. Fundamental and Applied Climatology, 8(1), 75–106 (In Russian), DOI: 10.21513/2410-8758-2022-1-75-106.

Serykh I. V. and Tolstikov A. V. (2022). Climate change in the western part of the Russian Arctic in 1980–2021. Part 2. Soil temperature, snow, and humidity. Problems of Arctic and Antarctic Research, 68(4), DOI: 10.30758/0555-2648-2022-68-3-258-277.

Si Z., Li. S., Huang L. and Chen Y. (2010). Visualization programming for batch processing of contour maps based on VB and Surfer software. Advances in Engineering Software, 41(7–8), 962–965.

Smirnov A. Yu. (2025). Northern Sea Route: output and prospects. Arctic: Ecology and Economy, 15(1), 109–118, (In Russian), DOI: 10.25283/2223-4594-2025-1-109-118.

The International Institute for Applied Systems Analysis (IIASA) and Russian Academy of Sciences (RAS), (2002). Land Resources of Russia. [online] Available at: http://www.iiasa.ac.at/Research/FOR/russia_cd/download.htm [Accessed 3 Nov. 2022].

Third Assessment Report on Climate Change and Its Consequences on the Territory of the Russian Federation: General Summary. Roshydromet (2022). St. Petersburg: Science-Intensive Technologies. 124 p., (In Russian).

Tolstykh M. A. (2016). Global atmosphere models: current state and development plans. Proceedings of the Hydrometeorological Research Center of the Russian Federation, 359, 5–32, (In Russian).

Yakubovich A. N. and Yakubovich I. A. (2019). Forecasting the impact of climatic changes on the functionality of the transport infrastructure of the permafrost zone in Russia. Intellect. Innovation. Investments, 1, 104–110, (In Russian).

Yang C. S., Kao S. P., Lee F. B. and Hung P. S. (2004). Twelve different interpolation methods: A case study of Surfer 8.0. In Proceedings of the XXth ISPRS Congress, Vol. 35, pp. 778–785.